การหานอร์แมลโคออร์ดิเนตด้วยวิธีนอนเฮสเซียน

นายจิระยุทธ สุปัญญาบุตร

NON-HESSIAN METHOD FOR NORMAL COORDINATES CALCULATION

Mr. Chirayut Supunyabut

จุฬาลงกรณ์มหาวิทยาลัย
CHULALONGKORN UNIVERSITY

A Thesis Submitted in Partial Fulfillment of the Requirements
for the Degree of Doctor of Philosophy Program in Chemistry
Department of Chemistry
Faculty of Science
Chulalongkorn University
Academic Year 2019
Copyright of Chulalongkorn University

Thesis Title	NON-HESSIAN METHOD FOR NORMAL COORDINATES CALCULATION
By	Mr. Chirayut Supunyabut
Field of Study	Chemistry
Thesis Advisor	Associate Professor Viwat Vchirawongkwin, Dr. rer. nat.

Accepted by the Faculty of Science, Chulalongkorn University in Partial Fulfillment of the Requirements for the Doctoral Degree

....Dean of the Faculty of Science

(Professor Dr. Polkit Sangvanich, Ph.D.)

THESIS COMMITTEE

....Chairman

(Associate Professor Dr. Vudhichai Parasuk, Ph.D.)

....Thesis Advisor

(Associate Professor Viwat Vchirawongkwin, Dr. rer. nat.)

....Examiner

(Professor Dr. Thawatchai Tuntulani, Ph.D.)

....Examiner

(Associate Professor Dr. Somsak Pianwanit, Ph.D.)

....External Examiner

(Associate Professor Chinapong Kritayakornupong, Dr. rer. nat.)

จิระยุทธ สุปัญญาบุตร : การหานอร์แมลโคออร์ดิเนตด้วยวิธีนอนเฮสเซียน. (NON-HESSIAN METHOD FOR NORMAL COORDINATES CALCULATION) อ.ที่ปรึกษาวิทยานิพนธ์หลัก : รศ.ดร.วิวัฒน์ วชิรวงศ์กวิน, 81 หน้า.

การวิเคราะห์หาความถี่ธรรมชาติมีบทบาทสำคัญในทางเคมีมาอย่างยาวนานโดยเป็นทั้งหัวใจสำคัญที่นำไปสู่ความเข้าใจการเคลื่อนที่เชิงโมเลกุล โดยเฉพาะอย่างยิ่งการสั่นของโมเลกุล และใช้บ่งชี้ลักษณะเฉพาะของพีกในอินฟราเรดและรามานสเปกตรัมได้ การวิเคราะห์หาความถี่ธรรมชาติแบบดั้งเดิมนั้นต้องเกี่ยวข้องกับการสร้างเฮเซียนเมทริกซ์และการประมาณค่าฮาร์มอนิกซึ่งแทบจะทำไม่ได้เลยเมื่อโมเลกุลมีขนาดใหญ่และใช้กับกลศาสตร์ควอนตัม งานวิจัยนี้นำเสนอวิธีการใหม่ที่ใช้สำหรับการคำนวณนอร์แมลโคออร์ดิเนตโดยใช้เพียงโครงสร้างเรขาคณิตของโมเลกุล อาศัยการพิจารณาโมเลกุลเป็นแบบโมเดลลูกบอลและแท่งร่วมกับการใช้การกระจายแบบอนุรักษ์ของโมเมนตัมเชิงมุมของเค้าโครงวัตถุแข็งเกร็ง วิธีการนี้เรียกว่าการกระจายโมเมนต์ความเฉื่อย (Expanded Moment of Inertia Tensor: **EMIT**) ตามวิธีที่ใช้สร้างขึ้นมา ข้อดีที่สำคัญของวิธีการนี้คือ สามารถหานอร์แมลโคออร์ดิเนตได้ทุกจุดบนพื้นผิวพลังงานศักย์และโหมดนอร์แมลที่ได้สอดคล้องกับที่ได้จากการคำนวณทางทฤษฎีซึ่งยืนยันจากการคำนวณสเปกตรัมกำลังของระบบไอออนลบ NO_2^- และ NO_3^- ในน้ำ งานวิจัยนี้ไม่ใช่แค่การนำเสนอวิธีทางเลือกเพื่อใช้หานอร์แมลโคออร์ดิเนตเท่านั้น แต่ยังเป็นการแสดงให้เห็นถึงวิธีการพิจารณาโลกกายภาพด้วยวิธีที่แตกต่างอีกด้วย

ภาควิชา..........เคมี.............. ลายมือชื่อนิสิต...

สาขาวิชา..........เคมี.............. ลายมือชื่อ อ.ที่ปรึกษาหลัก.......................................

ปีการศึกษา.......2562...........

5772807023 : MAJOR CHEMISTRY

KEYWORDS : Expanded Moment of Inertia Tensor/Normal Mode/vibration Mode

    CHIRAYUT SUPUNYABUT : NON-HESSIAN METHOD FOR NORMAL COORDINATES CALCULATION. ADVISOR : ASSOC. PROF. VIWAT VCHIRAWONGKWIN, Dr. rer. nat., 81 pp.

Normal mode analysis (NMA) plays an essential role in chemistry for a very long time. It is both a key to understanding molecular motions, especially vibration motions, and to identifying characteristic peaks in infrared and Raman spectra. The traditional NMA requires the construction of a Hessian matrix and using harmonic approximation, which is almost impossible when large molecules and quantum mechanics are involved. Usually, NMA serves a complete set of normal coordinates that describes all possible motion modes of a molecule. This work presents a novel methodology to calculate normal coordinates that use only molecular geometries as input by considering a molecule as a ball-and-stick model and using the conservative expansion of angular momentum within the rigid body framework. This method is named Expanded Moment of Inertia Tensor (**EMIT**) after the way it was created. The considerable advantages of the EMIT methodology are as follows: It can extract a complete set of normal coordinates from molecular geometry at any point in potential energy surface, and it provides normal modes that resemble those obtained from the theoretical calculation. The EMIT reliability was confirmed by calculations of power spectra of NO_2^- and NO_3^- anions in aqueous solutions. This is not only proposing an alternative method to calculate normal coordinates but also showing the way to consider physical worlds differently.

Department : ……..Chemistry….. Student's Signature ………………………………………

Field of Study : ….Chemistry….. Advisor's Signature ………………………………………

Academic Year : …2019…………

ACKNOWLEDGEMENTS

CONTENTS

LIST OF TABLES

LIST OF FIGURES

จุฬาลงกรณ์มหาวิทยาลัย

CHULALONGKORN UNIVERSITY

CHAPTER I

INTRODUCTION

1.1 Literature Review

Normal mode analysis (NMA) has been utilizing in vast scientific areas. For example, using normal modes in a 3D numerical simulation allows theoretical scientists to study p-mode damping of solar-like oscillating stars [1]. Astronomists used NMA to study of seismic waves of rubble-pile asteroids [2]. Seismologists were able to solve lots of seismological problems by developing a theoretical framework for the calculation of theoretical seismograms based on NMA [3, 4]. Biochemists and biologists could understand dynamic global characters of macromolecules, which play an essential role in explaining their functions [5–8]. Chemists might be familiar with the determination of infrared (IR) and Raman peaks obtained from spectroscopy instruments by using NMA [9–11].

The power spectrum typically refers to the Fourier transform of the autocorrelation function [12]. It is often used in signal processing to transform natural or observable signals into the frequency domain in many research fields such as electrical engineering, astronomy, cosmology, etc. In recent astronomy and cosmology research, Camera and co-workers developed an approach to optimize the utilization of angular power spectra with spectroscopic galaxy survey data [13]. Besides, Wilson and co-workers presented a forward modeling of the redshift-space power spectrum multipole moments for a masked density field that might provide constraints on modified gravity theories [14]. Meanwhile, in bio-medical research, Micarelli, with his team, used power spectra (PS) analysis to study the eye velocity traces of superior vestibular neuritis (VN) patients and healthy subjects that might

be used as a tool to monitor the patients [15].

During 2011 and 2014, a group of researchers led by Vchirawongkwin with co-workers studied dynamics behaviors of anions such as NO_2^-, NO_3^-, and CO_3^{2-} in aqueous solutions via quantum mechanical charge field (QMCF) molecular dynamics simulations. One interesting thing is that they computed the power spectra of those anions by using normal coordinates, velocity autocorrelation function (VACF) derived from the simulations, and Fourier transformation (FT). They found that the power spectra agreed with the experiments. However, at that time, they manually constructed normal coordinates by following the group theoretical methodology guidelines [16, 17].

In computational chemistry, especially molecular simulation, the alignment of the molecule for each simulation frame before analyzing is inescapable. The well-known methodology is using the principal axis of the moment of inertia as the reference axes. These can be found in most popular programs such as VMD and Gaussian [18, 19]. Usually, the principal axis is composed of three perpendicular vectors, which are computed by diagonalizing the moment of inertia tensor (MIT). However, the whole molecule must be considered as the single rigid body object, in other words, all atoms in a molecule are shrunk into one object.

Since the moment of inertia tensor combines all atoms in a molecule, vice versa, the key idea of this work is aiming to distribute the moment of inertia tensor to each atom by still keeping the molecule as the rigid body object. It is called an atomic moment of inertia tensor (AMIT). Each AMIT shares the same magnitude of angular velocity.

The MIT is always 3×3 matrix is now expanded to $3N \times 3N$ matrix where N is a number of atoms. The new matrix is called an expanded moment of inertia tensor (EMIT). Then, the complete set of normal coordinates is obtained by diagonalizing of this EMIT matrix and used for calculating power spectra as Vchirawongkwin and co-workers did in their works to validate its reliability.

CHAPTER II

THEORY

2.1 Normal Mode Analysis and Harmonic Approximation

2.1.1 Normal Mode Calculation

Consider a simple harmonic oscillator of a mass m connected with a spring that has a force constant k in one dimension (Figure **2.1**). According to Hooke's Law, The restoring force (F) can be calculated by:
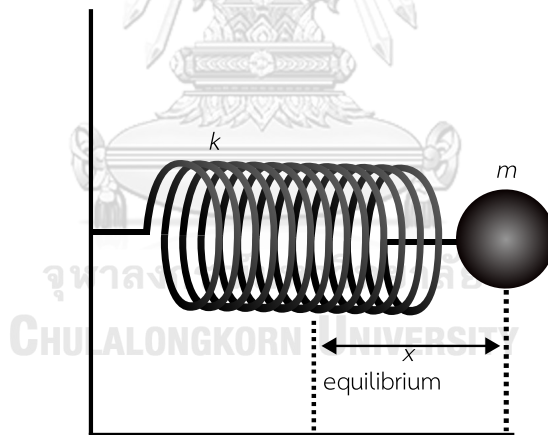
Figure **2.1**: A mass m is attached to a massless spring with constant k

$$F = -kx = -\frac{dV}{dx},$$ (2.1)

where the potential energy, $V = \frac{1}{2}kx^2$, and x is the distance from the equilibrium point.

In Newton's Law, the aforementioned force can also be calculated by $F = ma$. Thus, Equation (2.1) can be written as [20]

$$ma = -kx \quad \text{or} \quad m\frac{\partial^2 x}{\partial t^2} = -kx. \tag{2.2}$$

By solving the Newtonian equation, x is the function of time can be expressed as:

$$x(t) = A\sin(2\pi\nu t), \tag{2.3}$$

where t is time, ν is fundamental vibration frequency, and A is the amplitude of the vibration. Thus, Equation (2.2) will be

$$-4\pi^2\nu^2 mx = -kx. \tag{2.4}$$

The above equation shows the relationship between the force constant and the vibration frequency, which is elementary of normal modes calculations.

Usually, the force constant is an unknown variable, but it can be calculated by using the second derivative of the potential energy derived from Equation (2.1)

$$k = \frac{\partial^2 V}{\partial x^2}. \tag{2.5}$$

2.1.2 Harmonic Approximation

Consider the potential energy of an anharmonic oscillator in one dimension shown in Figure **2.2**. Near the minimum (x_0), the potential curve can be estimated by using a Taylor expansion as follow [21],
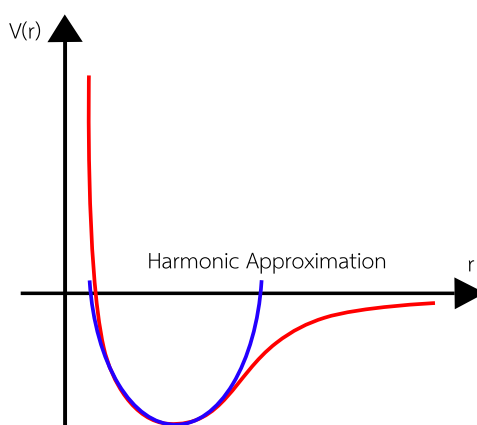
Figure **2.2**: The potential energy of an anharmonic oscillator as a function of internuclear distance (red) and the harmonic approximation (blue)

$$V(x) \approx V(x_0) + V'(x_0)(x-x_0) + \frac{1}{2!}V''(x_0)(x-x_0)^2 + ... + \frac{1}{n!}V^{(n)}(x_0)(x-x_0)^n. \quad (2.6)$$

Because the first term on the right is a constant, and the minimum can be set to 0 so that $V(x_0) = V(0) = 0$. The second term is also zero by definition of the derivation, leaving the third and higher terms in the equation. For harmonic approximation, terms with the power of 3 and higher are ignored, and the potential function is now called harmonic potential,

$$V(x) \approx \frac{1}{2!}V''(0)x^2 = \frac{1}{2}kx^2. \quad (2.7)$$

2.1.3 Normal Mode Analysis

In the Cartesian coordinate system, each atom in a molecule represented by the x-, y- and z-coordinates [20].

Atom i: $X_i, \quad Y_i, \quad Z_i.$

Let x_i, y_i, and z_i are the difference between the positions and equilibrium positions in the x-, y- and z- coordinates, respectively. The new extensions are:

Atom i: $x_i = X_i - X_{i,eq}$ $y_i = Y_i - Y_{i,eq}$ $z_i = Z_A - Z_{i,eq}$.

For a molecule consists of N atoms, there are $3N \times 3N$ possible force constants correspond to the motion of one atom subject to others. For example,

$$\frac{\partial V^2}{\partial x_1{}^2} = k_{xx}^{11} \tag{2.8}$$

is the force constant that represents the change of the force in the x-direction on atom 1 when it moves in the x-direction.

And,

$$\frac{\partial V^2}{\partial x_1 \partial y_1} = k_{xy}^{11} \tag{2.9}$$

is the force constant that represents the change of the force in the x-direction on atom 1 when it moves in the y-direction.

Likewise,

$$\frac{\partial V^2}{\partial x_1 \partial y_2} = k_{xy}^{12} \tag{2.10}$$

is the force constant that describes the change of the force in the x-direction on atom 1 when atom 2 moves in the y-direction. The $3N \times 3N$ matrix that composed of all possible force constants is called the Hessian matrix.

$$
\begin{pmatrix}
k_{xx}^{11} & k_{xy}^{11} & k_{xz}^{11} & k_{xx}^{12} & k_{xy}^{12} & k_{xz}^{12} & \cdots & k_{xx}^{1N} & k_{xy}^{1N} & k_{xz}^{1N} \\
k_{yx}^{11} & k_{yy}^{11} & k_{yz}^{11} & k_{yx}^{12} & k_{yy}^{12} & k_{yz}^{12} & \cdots & k_{yx}^{1N} & k_{yy}^{1N} & k_{yz}^{1N} \\
k_{zx}^{11} & k_{zy}^{11} & k_{zz}^{11} & k_{zx}^{12} & k_{zy}^{12} & k_{zz}^{12} & \cdots & k_{zx}^{1N} & k_{zy}^{1N} & k_{zz}^{1N} \\
k_{xx}^{21} & k_{xy}^{21} & k_{xz}^{21} & k_{xx}^{22} & k_{xy}^{22} & k_{xz}^{22} & \cdots & k_{xx}^{2N} & k_{xy}^{2N} & k_{xz}^{2N} \\
k_{yx}^{21} & k_{yy}^{21} & k_{yz}^{21} & k_{yx}^{22} & k_{yy}^{22} & k_{yz}^{22} & \cdots & k_{yx}^{2N} & k_{yy}^{2N} & k_{yz}^{2N} \\
k_{zx}^{21} & k_{zy}^{21} & k_{zz}^{21} & k_{zx}^{22} & k_{zy}^{22} & k_{zz}^{22} & \cdots & k_{zx}^{2N} & k_{zy}^{2N} & k_{zz}^{2N} \\
\vdots & \vdots & \vdots & \vdots & \vdots & \vdots & \ddots & \vdots & \vdots & \vdots \\
k_{xx}^{N1} & k_{xy}^{N1} & k_{xz}^{N1} & k_{xx}^{N2} & k_{xy}^{N2} & k_{xz}^{N2} & \cdots & k_{xx}^{NN} & k_{xy}^{NN} & k_{xz}^{NN} \\
k_{yx}^{N1} & k_{yy}^{N1} & k_{yz}^{N1} & k_{yx}^{N2} & k_{yy}^{N2} & k_{yz}^{N2} & \cdots & k_{yx}^{NN} & k_{yy}^{NN} & k_{yz}^{NN} \\
k_{zx}^{N1} & k_{zy}^{N1} & k_{zz}^{N1} & k_{zx}^{N2} & k_{zy}^{N2} & k_{zz}^{N2} & \cdots & k_{zx}^{NN} & k_{zy}^{NN} & k_{zz}^{NN}
\end{pmatrix}
\tag{2.11}
$$

Because of the force constants are calculated from the second derivative of the potential energy. All atoms in a molecule must be energy minimized to make sure that the molecule locates at the minimum in the potential energy surface where is the point that the harmonic approximation is valid.

2.2 Moment of Inertia Tensor

Consider a rigid body composed of N particles rotates with constant angular velocity ω around an axis that passes through its center of mass at the origin in Figure **2.3** [22].
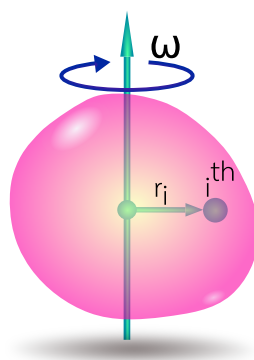
Figure **2.3**: A rigid rotating body

The total angular momentum can be expressed as

$$L = \sum_{i=1}^{N} m_i r_i \times \frac{\partial r_i}{\partial t} = \sum_{i=1}^{N} m_i r_i \times (\omega \times r_i) = \sum_{i=1}^{N} m_i [r_i^2 \omega - (r_i \cdot \omega) r_i], \quad (2.12)$$

where m_i and r_i are mass and position of an element i, respectively.

The above equation can be simply re-expressed in the matrix form

$$\begin{bmatrix} L_x \\ L_y \\ L_z \end{bmatrix} = \begin{bmatrix} I_{xx} & I_{xy} & I_{xz} \\ I_{yx} & I_{yy} & I_{yz} \\ I_{zx} & I_{zy} & I_{zz} \end{bmatrix} \begin{bmatrix} \omega_x \\ \omega_y \\ \omega_z \end{bmatrix}, \quad (2.13)$$

where

$$I_{xx} = \sum_{i=1}^{N} m_i (y_i^2 + z_i^2), \quad (2.14)$$

$$I_{yy} = \sum_{i=1}^{N} m_i (x_i^2 + z_i^2), \quad (2.15)$$

$$I_{zz} = \sum_{i=1}^{N} m_i (x_i^2 + y_i^2), \quad (2.16)$$

$$I_{xy} = I_{yx} = -\sum_{i=1}^{N} m_i (x_i y_i), \quad (2.17)$$

$$I_{yz} = I_{zy} = -\sum_{i=1}^{N} m_i (y_i z_i), \quad (2.18)$$

$$I_{xz} = I_{zx} = -\sum_{i=1}^{N} m_i (x_i z_i). \quad (2.19)$$

I_{xx}, I_{yy}, and I_{zz} are called the moment of inertia about the x-axis, y-axis, and z-axis, respectively. Meanwhile, I_{xy}, I_{yz}, and I_{xz} are the xy product of inertia, the yz product of inertia, and the xz product of inertia, respectively. Equation (2.13) can be represented as

$$L = I\omega, \quad (2.20)$$

where I is the moment of inertia, or rotational inertia, of a rigid body, which is the quantity that determines the mass is distributed about a rotation axis. Representing of I in the form of a matrix in Equation (2.13) is called the moment of inertia tensor (MIT).

2.3   Expanded Moment of Inertia Tensor

In the ball and stick model, a particular molecule can be considered as a quasi-rigid body that consists of N-point masses located at each center of its constituent atoms holding together by massless bonds (Figure **2.4**). The net angular momentum (L) of the molecule can be calculated by the product of the MIT (I) and the angular velocity (ω) as shown in Equation (2.20).
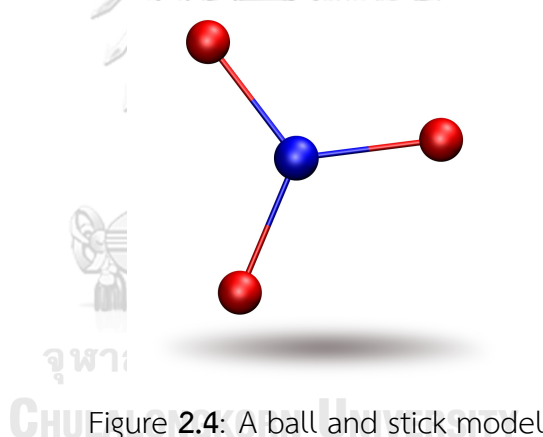
Figure **2.4**: A ball and stick model

The rigid body molecule rotates at the same angular velocity caused the total angular momentum is merely the total contribution from individual masses.

$$L = \sum_{a=1}^{N} l^a, \tag{2.21}$$

where l^a is an atomic angular momentum of each atom in the *N*-atom molecule that is defined as:

$$l^a = \iota^a \omega, \tag{2.22}$$

The atomic moment of inertia tensor (AMIT, ι^a) refers to the contribution of an

atom a to the MIT

$$\iota^a = m_a \begin{pmatrix} y_a^2 + z_a^2 & -x_a \cdot y_a & -x_a \cdot z_a \\ -y_a \cdot x_a & x_a^2 + z_a^2 & -y_a \cdot z_a \\ -z_a \cdot x_a & -z_a \cdot y_a & x_a^2 + y_a^2 \end{pmatrix}, \tag{2.23}$$

where the atom a can be regarded as a point mass m_a that resides at position (x_a, y_a, z_a) relative to the center of mass of the molecule.

By the multiplication of the identity, Equation (2.20) remains unchanged and can be rearranged as:

$$\begin{aligned}
\boldsymbol{L} &= \frac{N}{N} I \cdot \boldsymbol{\omega} \\
&= \left(\sum_{a=1}^{N} \frac{N}{N} \iota^a \right) \cdot \boldsymbol{\omega} \\
&= \sum_{a=1}^{N} \left(\frac{2-N}{N} + \frac{2N-2}{N} \right) \iota^a \cdot \boldsymbol{\omega}^a \qquad ; \boldsymbol{\omega}^a = \boldsymbol{\omega} \\
&= \sum_{a=1}^{N} \left[\frac{2-N}{N} \iota^a \cdot \boldsymbol{\omega}^a + \sum_{b=1}^{N} (1-\delta_{ab}) \frac{(\iota^a + \iota^b)}{N} \cdot \boldsymbol{\omega}^b \right] \\
&= \sum_{a=1}^{N} \underbrace{\sum_{b=1}^{N} \left[\delta_{ab} \frac{(2-N)}{N} \iota^a \cdot \boldsymbol{\omega}^a + (1-\delta_{ab}) \frac{(\iota^a + \iota^b)}{N} \cdot \boldsymbol{\omega}^b \right]}_{\lambda^a} \\
&= \sum_{a=1}^{N} \lambda^a,
\end{aligned} \tag{2.24}$$

where N is the number of atoms in the molecule. Although the term $\boldsymbol{\lambda}^a$ in Equation (2.24) looks very similar to the term $\boldsymbol{l}^a$ in Equation (2.21), it has a distinct definition. Since $\boldsymbol{l}^a$ is an individual angular momentum which means it does not take the interaction between atoms into account, but $\boldsymbol{\lambda}^a$ takes. The $\boldsymbol{\lambda}^a$ is named expanded angular momentum and is represented in a general form as:

$$\boldsymbol{\lambda}^a = \sum_{a=1}^{N} \phi^{ab} \cdot \omega^b. \tag{2.25}$$

The new term ϕ^{ab} can be defined as:

$$\boldsymbol{\phi}^{ab} = \begin{cases} \dfrac{2-N}{N}\boldsymbol{\iota}^a, & a = b \\ \dfrac{1}{N}(\boldsymbol{\iota}^a + \boldsymbol{\iota}^b), & a \neq b \end{cases}.$$

In tensor notation, we can conveniently write the definition as

$$\phi_{ij}^{ab} = \left(\frac{2-N}{N}\iota_{ij}^a\right) \cdot \delta^{ab} + \left(\frac{\iota_{ij}^a + \iota_{ij}^b}{N}\right) \cdot (1 - \delta^{ab}),$$

where i and j index the Cartesian basis (x, y, and z), in addition to the N-dimensional atomic labels a and b, and δ^{ab} is the Kronecker delta for the two atoms.

To define the *expanded moment of inertia tensor* (EMIT), we combine the two types of indices and represent this four-index mathematical object as a rank-two tensor

$$\Phi_{\mu\nu} = \Phi_{(ai)(bj)} = \phi_{ij}^{ab}.$$

The new labels μ and ν refer to the ith-axis of an atom a and j^{th}-axis of an atom b, therefore the EMIT matrix, $\boldsymbol{\Phi}$, is of $3N \times 3N$ dimension.

To understand how to construct the EMIT matrix and how to obtain the coefficient $2/N - 1$ and $1/N$ in Equation (2.24) clearly, more details will be discussed here. Firstly, each atomic moment of inertia (ι) will be divided into the N parts, which is now called a partial atomic moment of inertia tensor (PAMIT), where N is the number of atoms in the molecule,

$$\boldsymbol{\iota}^a = \sum_{a=1}^{N} \frac{1}{N}\iota^a. \tag{2.26}$$

The $i^{th}j^{th}$ off-diagonal element is constructed by the combination of the partial atomic moment of inertia tensors of an atom i and j. It allows the interaction of each atom is taken into account.

$$
\begin{pmatrix}
 & \frac{1}{N}(\iota^1 + \iota^2) & \frac{1}{N}(\iota^1 + \iota^3) & \cdots & \frac{1}{N}(\iota^1 + \iota^N) \\
\frac{1}{N}(\iota^2 + \iota^1) & & \frac{1}{N}(\iota^2 + \iota^3) & \cdots & \frac{1}{N}(\iota^2 + \iota^N) \\
\frac{1}{N}(\iota^3 + \iota^1) & \frac{1}{N}(\iota^3 + \iota^2) & & \cdots & \frac{1}{N}(\iota^3 + \iota^N) \\
\vdots & \vdots & \vdots & & \frac{1}{N}(\iota^4 + \iota^N) \\
\frac{1}{N}(\iota^N + \iota^1) & \frac{1}{N}(\iota^N + \iota^2) & \frac{1}{N}(\iota^N + \iota^3) & \frac{1}{N}(\iota^N + \iota^4) &
\end{pmatrix}
\tag{2.27}
$$

It is clearly seen that there are $2N - 2$ terms of $\frac{1}{N}\iota^{th}$ distribute to the matrix, $N - 1$ from i^{th} column, and $N - 1$ from i^{th} row. It is, therefore, $2 - N$ terms of $\frac{1}{N}\iota^{th}$ remain at diagonal elements of the matrix. The full $N \times N$ matrix is shown below.

$$
\begin{pmatrix}
\frac{2-N}{N}(\iota^1) & \frac{1}{N}(\iota^1 + \iota^2) & \frac{1}{N}(\iota^1 + \iota^3) & \cdots & \frac{1}{N}(\iota^1 + \iota^N) \\
\frac{1}{N}(\iota^2 + \iota^1) & \frac{2-N}{N}(\iota^2) & \frac{1}{N}(\iota^2 + \iota^3) & \cdots & \frac{1}{N}(\iota^2 + \iota^N) \\
\frac{1}{N}(\iota^3 + \iota^1) & \frac{1}{N}(\iota^3 + \iota^2) & \frac{2-N}{N}(\iota^3) & \cdots & \frac{1}{N}(\iota^3 + \iota^N) \\
\vdots & \vdots & \vdots & \ddots & \vdots \\
\frac{1}{N}(\iota^N + \iota^1) & \frac{1}{N}(\iota^N + \iota^2) & \frac{1}{N}(\iota^N + \iota^3) & \cdots & \frac{2-N}{N}(\iota^N)
\end{pmatrix}
\tag{2.28}
$$

Since ι is a 3×3 matrix, therefore, the matrix above is expanded to $3N \times 3N$ and re-written in simple form as:

$$
\begin{pmatrix}
\phi^{11} & \phi^{12} & \phi^{13} & \dots & \phi^{1N} \\
\phi^{21} & \phi^{22} & \phi^{23} & \dots & \phi^{2N} \\
\phi^{31} & \phi^{32} & \phi^{33} & \dots & \phi^{3N} \\
\vdots & \vdots & \vdots & \ddots & \vdots \\
\phi^{N1} & \phi^{N2} & \phi^{N3} & \dots & \phi^{NN}
\end{pmatrix}.
\tag{2.29}
$$

The crucial key of the EMIT methodology is that the eigenvectors matrix gained from the diagonalization of the $3N \times 3N$ EMIT matrix represents $3N$ normal coordinates of the molecule.

Equation (2.30) and (2.31) show the significant difference between $\boldsymbol{\lambda}^a$ and $\boldsymbol{l}^a$. In Equation (2.30), the total angular momentum is calculated by the dot product of a diagonal matrix of $\boldsymbol{l}^a$ and the atomic angular velocity matrix ω^a. In Equation (2.31), the total angular momentum is calculated by the multiplication of the EMIT matrix and the atomic angular velocity matrix.

$$
\boldsymbol{L} =
\begin{bmatrix}
l^1 & 0 & \dots & 0 \\
0 & l^2 & \dots & 0 \\
\vdots & \vdots & \ddots & \vdots \\
0 & 0 & \dots & l^N
\end{bmatrix}
\begin{bmatrix}
\omega_1 \\
\omega_2 \\
\vdots \\
\omega_N
\end{bmatrix},
\tag{2.30}
$$

$$
\boldsymbol{L} =
\begin{bmatrix}
\phi^{11} & \phi^{12} & \dots & \phi^{1N} \\
\phi^{21} & \phi^{22} & \dots & \phi^{2N} \\
\vdots & \vdots & \ddots & \vdots \\
\phi^{N1} & \phi^{N2} & \dots & \phi^{NN}
\end{bmatrix}
\begin{bmatrix}
\omega_1 \\
\omega_2 \\
\vdots \\
\omega_N
\end{bmatrix}.
\tag{2.31}
$$

2.4 Matrix Diagonalization

As mentioned in the previous section, the eigenvectors calculated from the diagonalization of the EMIT matrix represent all possible normal coordinates of the

molecule.

Generally, a particular matrix M is diagonalizable if it can be written as [23]:

$$M = P \cdot D \cdot P^{-1}, \tag{2.32}$$

where D is a diagonal matrix that consists of eigenvalues of M. Meanwhile, P is a nonsingular matrix that consists of eigenvectors corresponding to the eigenvalues in D, and P^{-1} is the matrix invert of P. To calculate P^{-1}, a matrix P must be a square matrix causing a matrix M also needs to be a square matrix. Moreover, all matrices M, D, P, and P^{-1} must have the same dimension. For a square matrix M that is symmetric, eigenvectors columns in P obtaining from the diagonalization are orthogonal vectors, which means the columns are perpendicular to each other. Since the EMIT matrix is a symmetric matrix, the normal vectors (eigenvectors) are orthogonal.

To compute eigenvalues and eigenvectors, let λ is a scalar, and it is said to be the eigenvalue of a square matrix A when there is a nontrivial solution satisfying the following equation [24].

$$AX = \lambda X, \tag{2.33}$$

where X is an eigenvector corresponding to λ.

Then, Equation (2.33) can be rearranged as follow

$$AX - \lambda X = 0$$
$$AX - \lambda I X = 0 \tag{2.34}$$
$$(A - \lambda I)X = 0,$$

since X must be a non-zero vector: thus, the characteristic polynomial of A

must equals to zero.

$$p(\lambda) = \det(A - \lambda I) = 0. \tag{2.35}$$

The following steps show an example of how to compute eigenvalues and eigenvectors.

Let A is a (2×2) square matrix.

$$A = \begin{bmatrix} 1 & -2 \\ 1 & 4 \end{bmatrix} \tag{2.36}$$

Then, the characteristic polynomial of A is

$$p(\lambda) = \det \begin{bmatrix} 1 - \lambda & -2 \\ 1 & 4 - \lambda \end{bmatrix}, \tag{2.37}$$

and

$$p(\lambda) = (1 - \lambda)(4 - \lambda) + 2 = \lambda^2 - 5\lambda + 6 = (\lambda - 2)(\lambda - 3). \tag{2.38}$$

Two eigenvalues of A are 2 and 3.

Consider an eigenvalue $\lambda = 2$, Equation 2.34 becomes

$$\left(\begin{bmatrix} 1 & -2 \\ 1 & 4 \end{bmatrix} - \begin{bmatrix} 2 & 0 \\ 0 & 2 \end{bmatrix} \right) \begin{bmatrix} X_1 \\ X_2 \end{bmatrix} = \begin{bmatrix} -1 & -2 \\ 1 & 2 \end{bmatrix} \begin{bmatrix} X_1 \\ X_2 \end{bmatrix} = 0. \tag{2.39}$$

Thus,

$$\begin{aligned} -X_1 - 2X_2 &= 0 \\ X_1 + 2X_2 &= 0 \end{aligned} \tag{2.40}$$

or

$$X_1 = -2X_2. \tag{2.41}$$

For convenient, let X_2 equals 1, hence, X_1 = -2 The eigenvector that corresponds to λ = 2 is

$$\begin{bmatrix} -2 \\ 1 \end{bmatrix}. \tag{2.42}$$

Consider an eigenvalue λ = 3, an Equation 2.34 becomes

$$\left(\begin{bmatrix} 1 & -2 \\ 1 & 4 \end{bmatrix} - \begin{bmatrix} 3 & 0 \\ 0 & 3 \end{bmatrix} \right) \begin{bmatrix} X_1 \\ X_2 \end{bmatrix} = \begin{bmatrix} -2 & -2 \\ 1 & 1 \end{bmatrix} \begin{bmatrix} X_1 \\ X_2 \end{bmatrix} = 0. \tag{2.43}$$

Thus,

$$\begin{aligned} -2X_1 - 2X_2 &= 0 \\ X_1 + X_2 &= 0 \end{aligned} \tag{2.44}$$

or

$$X_1 = -X_2. \tag{2.45}$$

Let X_2 equals 1, and X_1 = -1 The eigenvector that corresponds to λ = 3 is

$$\begin{bmatrix} -1 \\ 1 \end{bmatrix}. \tag{2.46}$$

Finally, eigenvalues are 2 and 3 and their corresponding eigenvectors are

$$\begin{bmatrix} -2 & -1 \\ 1 & 1 \end{bmatrix}. \tag{2.47}$$

Although the above example demonstrates an approach to compute eigenvalues and eigenvectors, it is usually used for small matrices. For larger matrices, there are several algorithms developed to reduce time-consuming. Meanwhile, their reliabilities are still acceptable such as the Jacobi algorithm, QR algorithm,

and spectral divide and conquer algorithms for real symmetric matrices and the combination between generalized Householder reflection and generalized QL algorithm for complex symmetric matrices.

This work uses the Eigen library package for C++ to deal with matrices [25]. The library provides real Schur decomposition to calculate eigenvectors and eigenvalues of real square matrices.

$$M = U \cdot D \cdot U^T, \qquad (2.48)$$

where U is a real orthogonal matrix, a matrix whose transpose equals its inverse, $U^{-1} = U^T$ and D is a real quasi-triangular matrix, a block-triangular matrix whose diagonal consists of 1-by-1 blocks and 2-by-2 blocks with complex eigenvalues. The diagonal elements of D are the eigenvalues of M. In general, there are both real and complex Schur decompositions, and this decomposition can compute eigenvalues and eigenvectors for square matrices that are not diagonalizable by Equation 2.32.

There are lots of applications of matrix diagonalization, such as calculation of normal coordinates from the EMIT matrix as described in Section 2.3, calculation of principal axes of inertia in Section 2.6. Moreover, it plays a vital role in solving a system of simultaneous linear differential equations, determining powers of matrices, and solving a system of differential equations, which is the key to quantum chemistry.

2.5   Pseudomolecular Model

According to the preliminary results, It was found that some of the normal vectors were not parallel or antiparallel to the bond direction as they should be. These were most often found in the symmetric stretching mode because of the nature of the EMIT that the normal vectors always point in or out from the center

of mass.
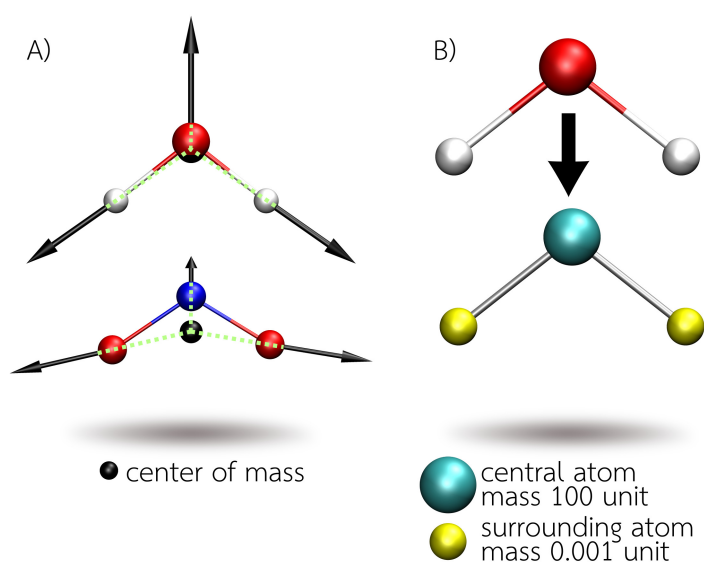
Figure **2.5**: (a) The symmetric stretching of a water molecule (top) and a nitrite anion (bottom) obtained from applying the EMIT method to actual molecules. The center of mass is shown in the black sphere/truncated sphere. (b) an approach to construct pseudomolecules

In this work, a pseudomolecule was used instead of an actual molecule. An approach to model a pseudomolecule is shown pictorially in Figure **2.5** and is described as follows: Firstly, all atoms in an actual molecule are changed to pseudoatoms. Secondly, pseudoatoms are divided into two types, which are a central atom and surrounding atoms. Thirdly, a mass of a central atom is set to 100 units; meanwhile, masses of surrounding atoms are set to 0.001 unit. Lastly, The pseudomolecule is used to construct the EMIT matrix instead of the actual molecule.

2.6   Reordering of Eigenvectors

Although eigenvectors obtained from diagonalization of the EMIT matrix represent a complete set of normal coordinates, there is no relationship between the sequences of eigenvectors with types of normal modes. The following steps were used to create a set of translation and rotational vectors as a set of reference vectors, and it will be used in separating of vibration modes out of other motion

modes.

2.6.1 Determine the Principal Axes of Inertia

Firstly, the center of mass (R_{COM}) of a molecule must be moved to the origin by:

$$r_{\text{coma}} = r_a - R_{\text{COM}}, \qquad (2.49)$$

where r_a is an initial coordinate and r_{coma} is an coordinate after shifting of the atom a and R_{COM} can be calculated by:

$$R_{\text{COM}} = \frac{\sum_a m_a r_a}{\sum_a m_a}. \qquad (2.50)$$

Secondly, the moment of inertia tensor (MIT) will be constructed as follow [19, 26]

$$\boldsymbol{I} = \begin{pmatrix} I_{xx} & I_{xy} & I_{xz} \\ I_{yx} & I_{yy} & I_{yz} \\ I_{zx} & I_{zy} & I_{zz} \end{pmatrix} = \begin{pmatrix} \sum_a m_a(y_a^2 + z_a^2) & \sum_a m_a(-x_a \cdot y_a) & \sum_a m_a(-x_a \cdot z_a) \\ \sum_a m_a(-y_a \cdot x_a) & \sum_a m_a(x_a^2 + z_a^2) & \sum_a m_a(-y_a \cdot z_a) \\ \sum_a m_a(-z_a \cdot x_a) & \sum_a m_a(-z_a \cdot y_a) & \sum_a m_a(x_a^2 + y_a^2) \end{pmatrix}.$$
$$(2.51)$$

Finally, the eigenvalues and eigenvectors are obtained from the diagonalization of MIT. The eigenvalues represent the principal moments; meanwhile, the 3×3 matrix of eigenvectors will be used to calculate the vectors corresponding to translation and rotation of the molecule in the upcoming step.

2.6.2   Construct a Matrix of Translation and Rotation Vectors

The three translation vectors (T_x, T_y, T_z), which correspond to translation in the x-, y-, and z-axis, respectively, are simply created by using the unit vectors [19].

For example, in the case of N atoms. The translation vectors that have $3N$ in dimension can be constructed by:

$$T_x = (1, 0, 0, 1, 0, 0, \cdots, 1, 0, 0)^T$$
$$T_y = (0, 1, 0, 0, 1, 0, \cdots, 0, 1, 0)^T$$
$$T_z = (0, 0, 1, 0, 0, 1, \cdots, 0, 0, 1)^T.$$

To construct the rotational vectors, let M is the eigenvectors obtained from the diagonalization of MIT.

$$\boldsymbol{M} = \begin{bmatrix} M_{11} & M_{12} & M_{13} \\ M_{21} & M_{22} & M_{23} \\ M_{31} & M_{32} & M_{33} \end{bmatrix}, \tag{2.52}$$

Firstly, The matrix M' is created by modification of the third column of the matrix M as follows

$$\boldsymbol{M'} = \begin{bmatrix} M_{11} & M_{12} & Cofactor\,M_{13} \\ M_{21} & M_{22} & -1 \cdot Cofactor\,M_{23} \\ M_{31} & M_{32} & Cofactor\,M_{33} \end{bmatrix}, \tag{2.53}$$

Secondly, the dot product between M'^T and the coordinates of the atom a concerning the center of mass gives

$$(x'_a, y'_a, z'_a)^T = M'^T \cdot (x_a, y_a, z_a).$$

Finally, The three rotational vectors (R_x, R_y, R_z), which correspond to rotation in the x-, y-, and z-axis, respectively, can be expressed as follows.

$$R_{x,i} = \begin{pmatrix} \sqrt{m_1}(y'_1 M'_{31} - z'_1 M'_{21}) \\ \sqrt{m_1}(y'_1 M'_{32} - z'_1 M'_{22}) \\ \sqrt{m_1}(y'_1 M'_{33} - z'_1 M'_{23}) \\ \sqrt{m_2}(y'_2 M'_{31} - z'_2 M'_{21}) \\ \sqrt{m_2}(y'_2 M'_{32} - z'_2 M'_{22}) \\ \sqrt{m_2}(y'_2 M'_{33} - z'_2 M'_{23}) \\ \vdots \\ \sqrt{m_3}(y'_3 M'_{31} - z'_3 M'_{21}) \\ \sqrt{m_3}(y'_3 M'_{32} - z'_3 M'_{22}) \\ \sqrt{m_3}(y'_3 M'_{33} - z'_3 M'_{23}) \end{pmatrix},$$

$$R_{y,i} = \begin{pmatrix} \sqrt{m_1}(z'_1 M'_{11} - x'_1 M'_{31}) \\ \sqrt{m_1}(z'_1 M'_{12} - x'_1 M'_{32}) \\ \sqrt{m_1}(z'_1 M'_{13} - x'_1 M'_{33}) \\ \sqrt{m_2}(z'_2 M'_{11} - x'_2 M'_{31}) \\ \sqrt{m_2}(z'_2 M'_{12} - x'_2 M'_{32}) \\ \sqrt{m_2}(z'_2 M'_{13} - x'_2 M'_{33}) \\ \vdots \\ \sqrt{m_3}(z'_3 M'_{11} - x'_3 M'_{31}) \\ \sqrt{m_3}(z'_3 M'_{12} - x'_3 M'_{32}) \\ \sqrt{m_3}(z'_3 M'_{13} - x'_3 M'_{33}) \end{pmatrix},$$

$$R_{z,i} = \begin{pmatrix} \sqrt{m_1}(x'_1 M'_{21} - y'_1 M'_{11}) \\ \sqrt{m_1}(x'_1 M'_{22} - y'_1 M'_{12}) \\ \sqrt{m_1}(x'_1 M'_{23} - y'_1 M'_{13}) \\ \sqrt{m_2}(x'_2 M'_{21} - y'_2 M'_{11}) \\ \sqrt{m_2}(x'_2 M'_{22} - y'_2 M'_{12}) \\ \sqrt{m_2}(x'_2 M'_{23} - y'_2 M'_{13}) \\ \vdots \\ \sqrt{m_3}(x'_3 M'_{21} - y'_3 M'_{11}) \\ \sqrt{m_3}(x'_3 M'_{22} - y'_3 M'_{12}) \\ \sqrt{m_3}(x'_3 M'_{23} - y'_3 M'_{13}) \end{pmatrix},$$

where m_i is the mass of an atom i^{th}. Please note that the dimension of each rotational vector is the same as the dimension of translation vectors.

$$
\begin{array}{cccccc}
T_x & T_y & T_z & R_x & R_y & R_z
\end{array}
$$

$$
\begin{pmatrix}
T_{1,x} & T_{1,y} & T_{1,z} & R_{1,x} & R_{1,y} & R_{1,z} \\
T_{2,x} & T_{2,y} & T_{2,z} & R_{2,x} & R_{2,y} & R_{2,z} \\
T_{3,x} & T_{3,y} & T_{3,z} & R_{3,x} & R_{3,y} & R_{3,z} \\
T_{4,x} & T_{4,y} & T_{4,z} & R_{4,x} & R_{4,y} & R_{4,z} \\
\vdots & \vdots & \vdots & \vdots & \vdots & \vdots \\
T_{3N,x} & T_{3N,y} & T_{3N,z} & R_{3N,x} & R_{3N,y} & R_{3N,z}
\end{pmatrix}
$$

The scoring function for the translation mode in the i direction with the column j^{th} of the normal coordinates matrix (N) can be expressed as:

$$
ST = \left| \sum_{i=k}^{3N} T_{i,k} \cdot N_{j,k} \right|, \tag{2.54}
$$

since the T_i and N_j are normalized, the maximum value must equal to 1, which means that N_j is most similar to T_i. In contrast, the 0 value means there is no relationship between N_j and T_i.

After the three translation modes were removed from the normal coordinates matrix (N), the remaining were compared with the reference rotational vectors using the following scoring function,

$$
SR = \left| \sum_{i=k}^{3N} R_{i,k} \cdot N_{j,k} \right|. \tag{2.55}
$$

The interpretation of the score is the same as in the translation scoring function. Then, the remaining $3N - 6$ columns of the normal coordinates matrix, for non-linear molecules, are now the vibration modes.

2.7 Quantum Mechanical Charge Field Molecular Dynamics (QMCF MD)

The principle of quantum mechanical charge field (QMCF) molecular dynamics lies in the quantum mechanical/molecular mechanical (QM/MM) dynamics which the simulation system is divided into two main regions that are quantum mechanical (QM) region and molecular mechanical (MM) region [27]. The significant difference is that, in the QMCF, the QM region is now divided into two subregions, QM core zone, and QM solvation layer. These following equations calculate the forces acting on a particle J located in each region,
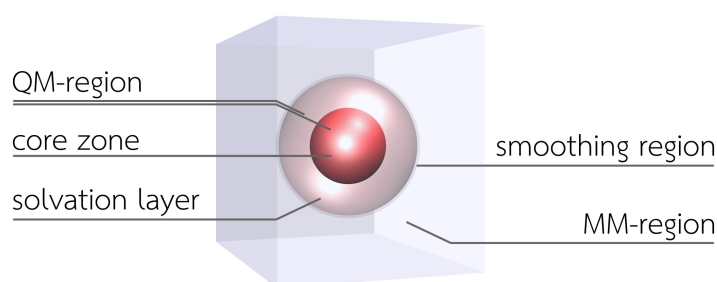
Figure **2.6**: Definition of quantum mechanical and molecular mechanical regions in the QMCF approach

$$\boldsymbol{F}_J^{core} = F_J^{QM}, \tag{2.56}$$

$$\boldsymbol{F}_J^{layer} = F_J^{QM} + \sum_{I=1}^{M} F_{IJ}^{BJHnC}, \tag{2.57}$$

$$\boldsymbol{F}_J^{MM} = \sum_{I=1,I \neq J}^{M} F_{IJ}^{BJH} + \sum_{I=1}^{N_1+N_2} \frac{q_I^{QM} \cdot q_J^{QM}}{r_{IJ}^2} + \sum_{I=1}^{N_2} F_{IJ}^{BJHnC}, \tag{2.58}$$

where F_J^{core} represents quantum mechanical forces acting on particle J in the

core zone, F_J^{layer} is the forces acting on particles J in the solvation layer, and F_J^{MM} corresponds to the forces acting on particles J located in the MM region.

2.8   Evaluation of Power Spectra

In general, the velocity autocorrelation function (VACF) and Fourier transform (FT) are used to calculate power spectra of molecules. This traditional method provides one power spectra for one molecule because there is only one velocity trajectory. In this work, normal modes analysis is added up in order to calculate an individual power spectra that corresponds to each normal coordinate.

2.8.1   Normal Coordinates

Normal mode analysis usually provides a complete set of normal coordinates that used to create normal modes. In this work, The normal coordinates, Θ , are the eigenvectors matrix and can be automatically calculated by the diagonalization of the EMIT matrix constructed by using a pseudomolecule. For N atoms system, the normal coordinates can be represented as:

$$\Theta = (|\theta_1\rangle, |\theta_2\rangle, \cdots, |\theta_{3N}\rangle), \tag{2.59}$$

2.8.2   Velocity Autocorrelation Function (VACF)

The normalized velocity autocorrelation function of the mode q^{th} is defined as

$$C_q(t) = \frac{\sum_i^{n_t} \langle v_q(t_i)|v_q(t_i+t)\rangle}{\sum_i^{n_t} \langle v_q(t_i)|v_q(t_i)\rangle}, \tag{2.60}$$

where n_t is the number of time origins t_i, $|v_q(t_i)\rangle$ and $|v_q(t_i+t)\rangle$ are the velocity vectors expressing the vibration mode q at time t_i and $t_i + t$, respectively.

The definition of velocity vectors above is quite different from the atomic velocities in molecular dynamic simulation.

Let $\mathbb{V}$ is the atomic velocity

$$\mathbb{V} \equiv \begin{pmatrix} v_x^1 & v_y^1 & v_z^1 & v_x^2 & \dots & v_z^N \end{pmatrix}^T,$$

Then, $\mathbb{V}$ is projected onto the normal coordinate basis

$$\mathbb{U} = \begin{pmatrix} u_1 & u_2 & \dots & u_{3N} \end{pmatrix}^T = \mathbf{\Theta}^T \mathbb{V}.$$

Finally, scale the normal coordinate basis by its corresponding velocities,

$$|v_q\rangle = u_q |\theta_q\rangle.$$

The methodology to evaluate power spectra is summarized in Figure **2.7**. Begin with choosing the atomic positions from the MD simulation. For convenient, the atomic positions were taken from the first step to construct the pseudomolecule. Then calculate the EMIT matrix and diagonalize it to obtain the eigenvector matrix, which is a complete set of normal coordinates, then calculate the velocity vector of each simulation step. Lastly, a series of velocity vectors were converted to power spectra by Fourier transformation.
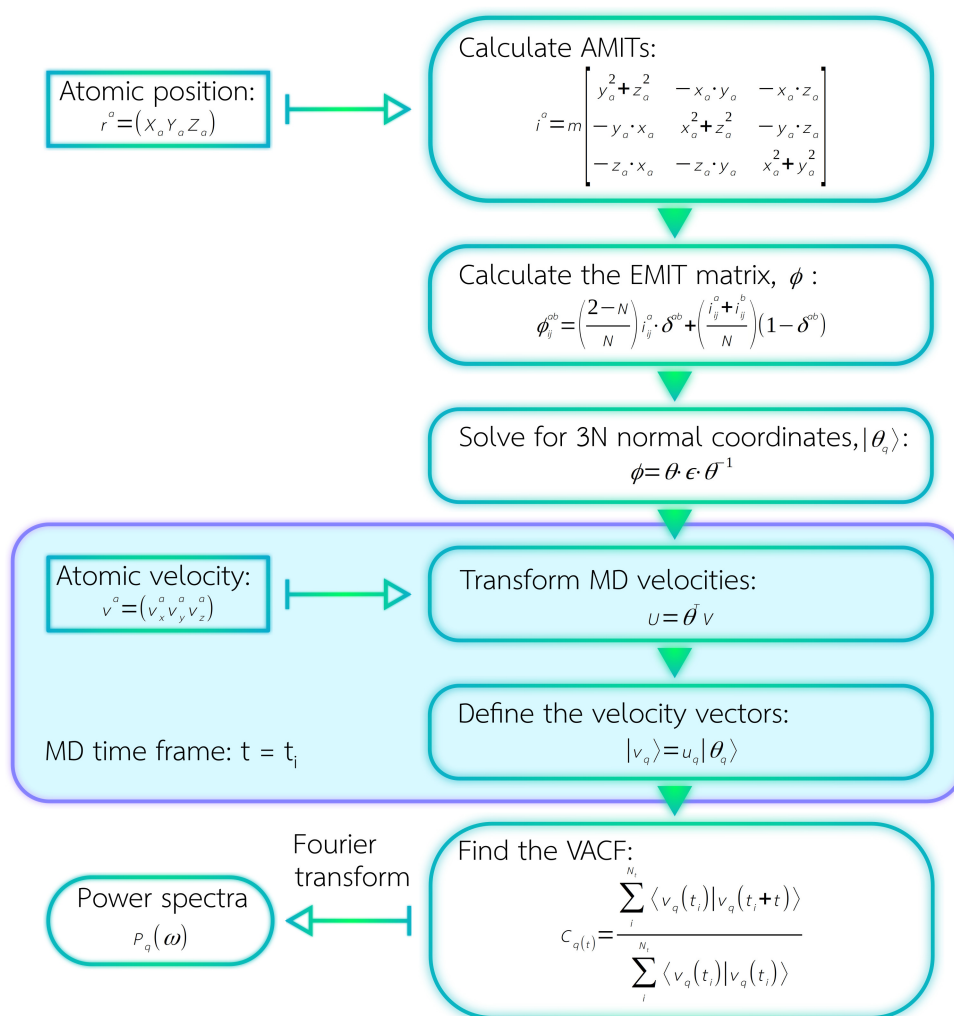
Figure **2.7**: Schematic diagram showing steps in the computation of power spectra, using the EMIT method, from MD simulation.

2.8.3 Fourier Transform

Continuous Fourier Transform: The Fourier Transform is a mathematical tool that decomposes any waveform, a representation of any variables as a function of time, space, etc., into a sum of sinusoidal basis functions [28]. Given $g(t)$ is the continuous function of time (t), the Fourier Transform of the function $g(t)$ is

$$\mathbb{F}_t[g(t)](f) = G(f) = \int_{-\infty}^{\infty} g(t)e^{-2\pi ift}dt, \tag{2.61}$$

where $G(f)$ is called the spectrum of g, which is a function of frequency (f). The above equation is called the forward Fourier transform. Conversely, $G(f)$ can be converted back to $g(t)$ by following equation.

$$\mathbb{F}_f^{-1}[G(f)](t) = g(t) = \int_{-\infty}^{\infty} G(f)e^{2\pi ift}df, \tag{2.62}$$

which is called the inverse Fourier transform.

According to Euler's formula, $e^{ix} = \cos(x) + i\sin(x)$, the complex exponential function inside the integral can be split into sine and cosine terms. Thus, the Fourier transform can also be expressed in terms of the Fourier sine transform and Fourier cosine transform, as shown below.

$$\mathbb{F}_t[g(t)](f) = G(f) = \int_{-\infty}^{\infty} E(t)\cos(2\pi ift)dt - i\int_{-\infty}^{\infty} O(t)\sin(2\pi ift)dt, \tag{2.63}$$

where $E(t)$ and $O(t)$ are even and odd portions, respectively, the first term is often called a real part of the full complex Fourier transform. Meanwhile, another term is called an imaginary part.

Discrete Fourier Transform: So far $g(t)$ is defined as a continuous function. Now, consider the case of a discrete function. Let $g(k)$ is one in N sample points taken from $g(t)$. It can be denoted as $g(0)$, $g(1)$, $g(2)$, ..., $g[N-1])$. The discrete Fourier transform (DFT) can be defined as [29, 30]:

$$\mathbb{F}_n[\{g(k)\}_{k=0}^{N-1}](n) = G(n) = \sum_{k=0}^{N-1} g(k)e^{-2\pi ink/N}, \tag{2.64}$$

where $G(n)$ is the nth frequency bin, and its frequency resolution can be calculated by the division of sampling frequency by the number of samples.

And the inverse discrete Fourier transform is

$$\mathbb{F}_n^{-1}[\{G(n)\}_{n=0}^{N-1}](k) = g(k) = \frac{1}{N}\sum_{n=0}^{N-1}G(n)e^{2\pi ink/N}. \tag{2.65}$$

Usually, if a sequence of $g(k)$ is real numbers, a sequence of $G(n)$ obtained from DFT will have the same length with a sequence of $g(k)$ and is complex numbers causing $G(n)$ and $G(N-n)$ have the same value. Thus, the frequencies that can be used for analyzing are in between 0 Hz to (sampling frequency)/2 Hz. In other words, the sampling frequency must be at least twice the highest waveform frequency to make sure that the calculated frequency will appear within (sampling frequency)/2 Hz, which is called Nyquist Frequency. Moreover, plotting the magnitude of $G(n)$ versus frequency is called a power spectrum.

To demonstrate how DFT works, let consider a sequence of 4 samples data ($N = 4$) collected with sampling frequency 4 Hz. The value of $g_{(0)}$, $g_{(1)}$, $g_{(2)}$, and $g_{(3)}$ are g_0, g_1, g_2, and g_3, respectively.

Since sampling frequency = 4 Hz and a number of samples are 4. Thus, the frequency resolution is calculated by

$$\text{frequency resolution} = \frac{4\,\text{Hz}}{4} = 1\,\text{Hz}, \tag{2.66}$$

and the value for the first frequency bin $G_{(0)}$ (0 Hz) is

$$G_{(0)} = g_0 \cdot e^{-2\pi i(0)(0)/(4)} + g_1 \cdot e^{-2\pi i(0)(1)/(4)} + g_2 \cdot e^{-2\pi i(0)(2)/(4)} + g_3 \cdot e^{-2\pi i(0)(3)/(4)}. \tag{2.67}$$

Like wise, the value for the frequency bin $G_{(1)}$ (1 Hz) is

$$G_{(1)} = g_0 \cdot e^{-2\pi i(2)(1)/(4)} + g_1 \cdot e^{-2\pi i(1)(1)/(4)} + g_2 \cdot e^{-2\pi i(1)(2)/(4)} + g_3 \cdot e^{-2\pi i(1)(3)/(4)}, \quad (2.68)$$

$G_{(2)}$ (2 Hz) and $G_{(3)}$ (3 Hz) can be calculated using the same procedure. Furthermore, the Nyquist Frequency is 2 Hz.

CHAPTER III

METHOD

3.1 Obtaining of Normal Coordinates

To obtain the complete set of normal coordinates, Three compounds, H_2O, NO_2^- and NO_3^-, were used as examples. The molecules were geometry optimized at the MP2 level with the 6-311++G(d,p) basis set. These compounds, then, were used to construct EMIT matrices. All calculations are shown in Table **3.1**.

Table **3.1**: EMIT methodology to calculate normal coordinates

Calculation	Add on*		
	H_2O	NO_2^-	NO_3^-
1	EMIT	EMIT	EMIT
2	EMIT+PMM+RO	EMIT+PMM+RO	EMIT+PMM+RO

*EMIT is the EMIT methodology, PMM is the pseudo-molecular model and RO is the reordering of eigenvectors.

3.2 Obtaining of Power Spectrum

This work took the outputs from the same simulations in Vchirawongkawin's works [16, 17]. Details of their work are briefly described as follows. The simulations of NO_2^- and NO_3^- anions in aqueous solutions were carried out on quantum mechanical charge field molecular dynamics (QMCF MD) that counting the N-body effects into the dynamical properties of the solute.

Parameters were specifically chosen in order to keep the density of the cubic box resembles the experimental value, which is 0.997 g cm^{-1} at 298 K in pure water. Some important parameters are listed in Table **3.2**. The temperature was preserved

at 298.16 K by the Berenden temperature scaling algorithm with a relaxation time of 100 fs. The simulations were performed with the time step of 0.2 fs under the NVT-ensemble using a predictor-corrector algorithm and were kept running for 50,000 steps (10 ps). The output is written after every five steps. Thus there are 10,000 steps for output, and the step size is 1.0 fs.

Table **3.2**: The simulation parameters for each simulation system

Parameters	Simulation System	
	Nitrite [16]	Nitrate [17]
Number of solutes	1	1
Number of water	496	496
Box length (Å)	24.64	24.65
Temperature (K)	298	298
Core radius (Å)	3.2	3.5
QM radius (Å)	6.8	6.8

The details to calculate the power spectra are adapted from Vchirawongkawin's works and will be described in Figure **3.1** as follow. Firstly, in the 10,000 steps (10 ps), the coordinates of the first step were used to calculate normal coordinates. Please be reminded that in Vchirawongkawin's works, they recalculated normal coordinates for every step. Secondly, all atomic velocities are transformed to the normal coordinate basis. At this step, one set of atomic velocities was expanded to $3N$ sets correspond to each mode in the normal coordinates. Thirdly, the newly defined velocities were used to calculate the velocity autocorrelation. The length of the velocity autocorrelation function is 1000 steps, and the newly defined velocity at the first step and every five steps, later on, were used as the references. Each segment of the velocity autocorrelation functions was averaged into one sequence. Since data points obtained from VACF is a half sinusoidal waveform with 90° phase (cosine waveform), thus, a sequence of data points must be extended before calculate power spectra using DFT making it the full waveform with 0° phase (sine waveform) by the following equation.

$$\sum_{n=1}^{2N-1} g'_{(n)} = \begin{cases} g_{(N-n+1)} & ; n < N \\ g_{(n-N+1)} & ; n \geqslant N, \end{cases} \tag{3.1}$$
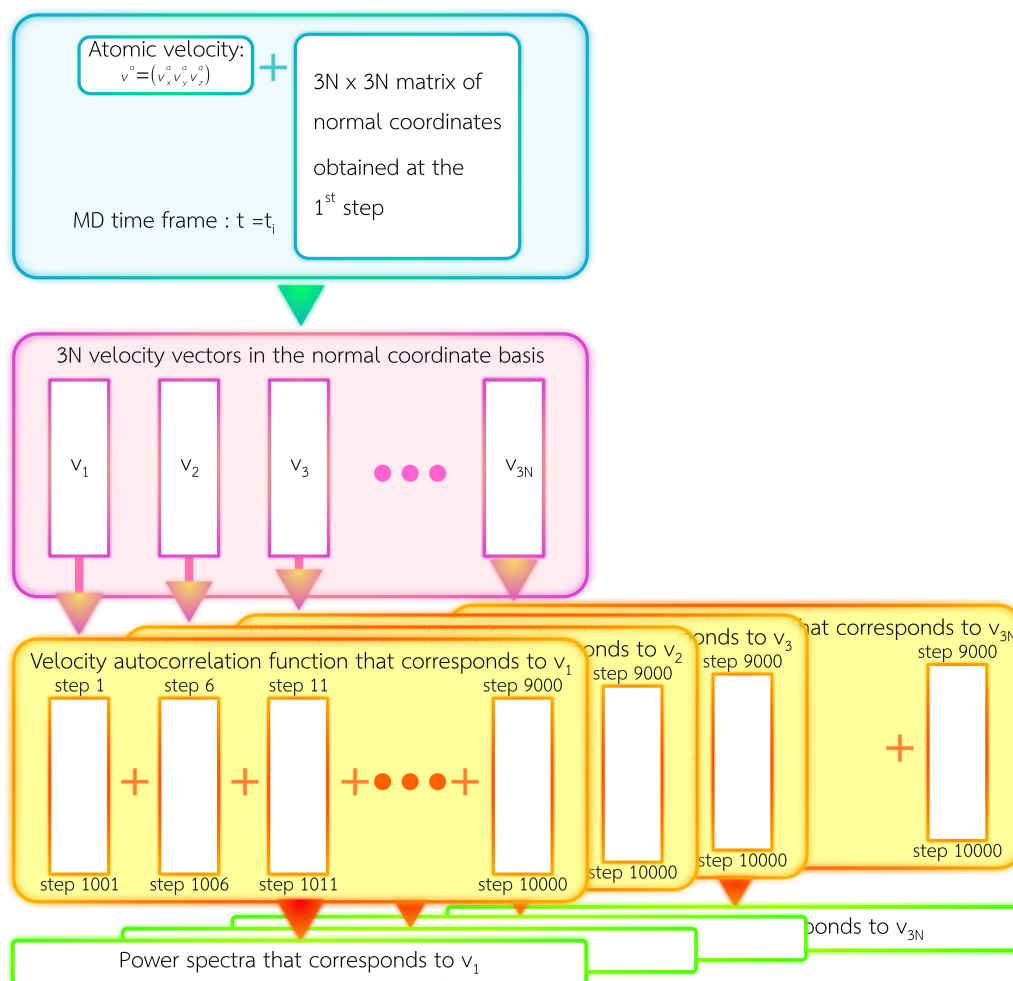
Figure **3.1**: An approach to calculate VACF

where $g_{(n)}$ and $g'_{(n)}$ are original VACF and extended VACF , respectively. Since there are 10,000 steps for 10 ps, the sampling frequency is 1.0×10^{15} Hz. According to Equation 3.1, there are 1,999 data points. The frequency resolution in cm^{-1} is 1.0×10^{15} $s^{-1}/(1,999 \times 2.99792458 \times 10^{-10}$ $cm/s^{-1}) = 16.6865$ Hz

Finally, Using discrete Fourier transformation to transform $3N$ velocity autocorrelation functions into $3N$ spectra.

3.3   Implementation

Construction of EMIT matrices and calculation of normal coordinates and power spectra were implemented in C++ with the Eigen library [25].

CHAPTER IV

RESULTS AND DISCUSSION

4.1   EMIT Methodology and Normal Coordinates

To study the EMIT methodology and to obtain a set of normal coordinates, a water molecule was first used as an example.

Firstly, a model of a water molecule was constructed and geometry optimized, as described in Section 3.1. Positions of each atom are shown in Table **4.1**.

Table **4.1**: Coordinates of a water molecule in Angstrom after geometry optimization.

Atom	x	y	z
O	0.0000	0.0000	0.1188
H1	0.0000	0.7534	−0.4754
H2	0.0000	−0.7534	−0.4754

Secondly, the whole molecule was translated to move the center of mass to the origin (0, 0, 0) before starting to construct the AMIT in Equation (2.23). An AMIT of each atom is shown in Table **4.2**.

Thirdly, the 9×9 matrix was constructed by an equation (2.28). The matrix is shown in Table **4.3**.

Finally, the eigenvectors and eigenvalues were obtained after the diagonalization of the EMIT matrix. The eigenvalues and corresponding eigenvectors are shown in Table **4.4**.

Table **4.2**: An AMIT of each atom in the water molecule

Atom	AMIT		
O	0.0708	0.0000	0.0000
	0.0000	0.0708	0.0000
	0.0000	0.0000	0.0000
H1	0.8528	0.0000	0.0000
	0.0000	0.2807	0.4008
	0.0000	0.4008	0.5721
H2	0.8528	0.0000	0.0000
	0.0000	0.2807	$-$0.4008
	0.0000	$-$0.4008	0.5721

Table **4.3**: The EMIT matrix of the water molecule

−0.0236	0.0000	0.0000	0.3079	0.0000	0.0000	0.3079	0.0000	0.0000
0.0000	−0.0236	0.0000	0.0000	0.1172	0.1336	0.0000	0.1172	−0.1336
0.0000	0.0000	0.0000	0.0000	0.1336	0.1907	0.0000	−0.1336	0.1907
0.3079	0.0000	0.0000	−0.2843	0.0000	0.0000	0.5685	0.0000	0.0000
0.0000	0.1172	0.1336	0.0000	−0.0936	−0.1336	0.0000	0.1872	0.0000
0.0000	0.1336	0.1907	0.0000	−0.1336	−0.1907	0.0000	0.0000	0.3814
0.3079	0.0000	0.0000	0.5685	0.0000	0.0000	−0.2843	0.0000	0.0000
0.0000	0.1172	−0.1336	0.0000	0.1872	0.0000	0.0000	−0.0936	0.1336
0.0000	−0.1336	0.1907	0.0000	0.0000	0.3814	0.0000	0.1336	−0.1907

Table **4.4**: The eigenvalues and corresponding eigenvectors of the water molecule

column	1	2	3	4	5	6	7	8	9
eigenvalues	−0.3314	0.5921	0.3814	−0.4714	0.0000	−0.8528	0.2107	−0.6727	−0.0401
eigenvectors	−0.8165	0.5774	0.0000	0.0000	0.0000	0.0000	0.0000	0.0000	0.0000
	0.0000	0.0000	0.0000	0.0000	0.0000	0.0000	−0.5774	0.3257	0.7487
	0.0000	0.0000	−0.5774	−0.5193	0.6301	0.0000	0.0000	0.0000	0.0000
	0.4082	0.5774	0.0000	0.0000	0.0000	0.7071	0.0000	0.0000	0.0000
	0.0000	0.0000	0.0000	0.5457	0.4497	0.0000	−0.5774	−0.1628	−0.3744
	0.0000	0.0000	−0.5774	0.2596	−0.3150	0.0000	0.0000	−0.6484	0.2820
	0.4082	0.5774	0.0000	0.0000	0.0000	−0.7071	0.0000	0.0000	0.0000
	0.0000	0.0000	0.0000	−0.5457	−0.4497	0.0000	−0.5774	−0.1628	−0.3744
	0.0000	0.0000	−0.5774	0.2596	−0.3150	0.0000	0.0000	0.6484	−0.2820

The sets of normal coordinates are projected onto the water molecule and pictorial displayed in Figure **4.1** by the sequence of output from the matrix diagonalization.

Figure **4.1**: Nine normal coordinates of a water molecule that could be identified as following modes, T_q represents translation in the q-direction, R_q represents rotation around the q-axis, v_s is the symmetric stretching, v_{as} is the anti-symmetric stretching, and σ is the bending modes.

Theoretically, a water molecule has nine motion modes, including three translation, three rotation, and three vibration modes. The three vibration modes are divided into a symmetric stretching, an anti-symmetric stretching, and a bending mode. According to Figure **4.1**, it is obvious that the normal coordinates obtained from the EMIT methodology could represent the directions of motions of the water molecule. The translation in the x-axis, y-axis, and z-axis are modes 2, 8, and 3, respectively. The rotation around the x-axis, y-axis, and z-axis are modes 7, 1, and, 6, respectively. Modes 4, 5, and 9 are bending, symmetric stretching, and

anti-symmetric stretching modes, respectively.

Interestingly, it is also found that three normal coordinates that resemble the translation modes have positive eigenvalues. Meanwhile, those that have significant negative eigenvalues resemble the rotation modes. The eigenvalues of the normal coordinates that represent the vibration modes are in between those of translation and rotation.

More investigations were carried out by using NO_2^- and NO_3^- anions (full data could be found in an Appendix A).

Figure **4.2**: Nine normal coordinates of an NO_2^- molecule that could be identified as following modes, T_q represents translation in the q-direction, R_q represents rotation around the q-axis, v_s is the symmetric stretching, v_{as} is the anti-symmetric stretching, and σ is the bending modes.

Figure **4.2** shows the projection of nine normal coordinates to the NO_2^- anion. Sets of normal coordinates could be identified as follow: translation in the x-direction, rotation around the y-axis, translation in the y-direction, anti-symmetric stretching, rotation around the x-axis, translation in the z-direction, rotation around the z-axis, bending and symmetric stretching.
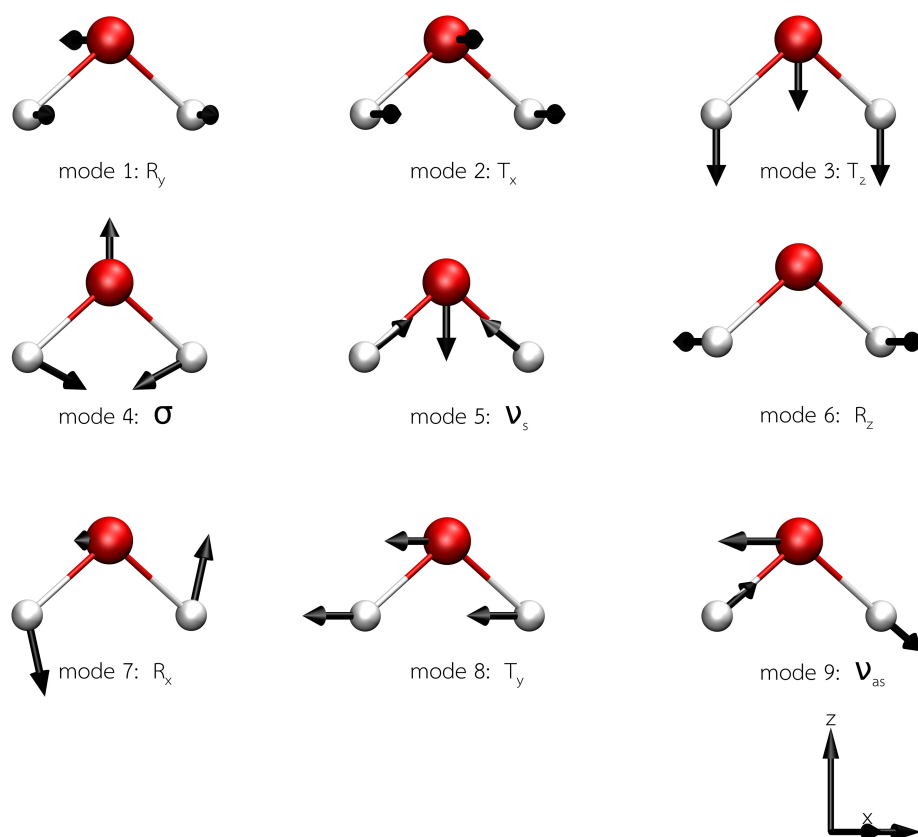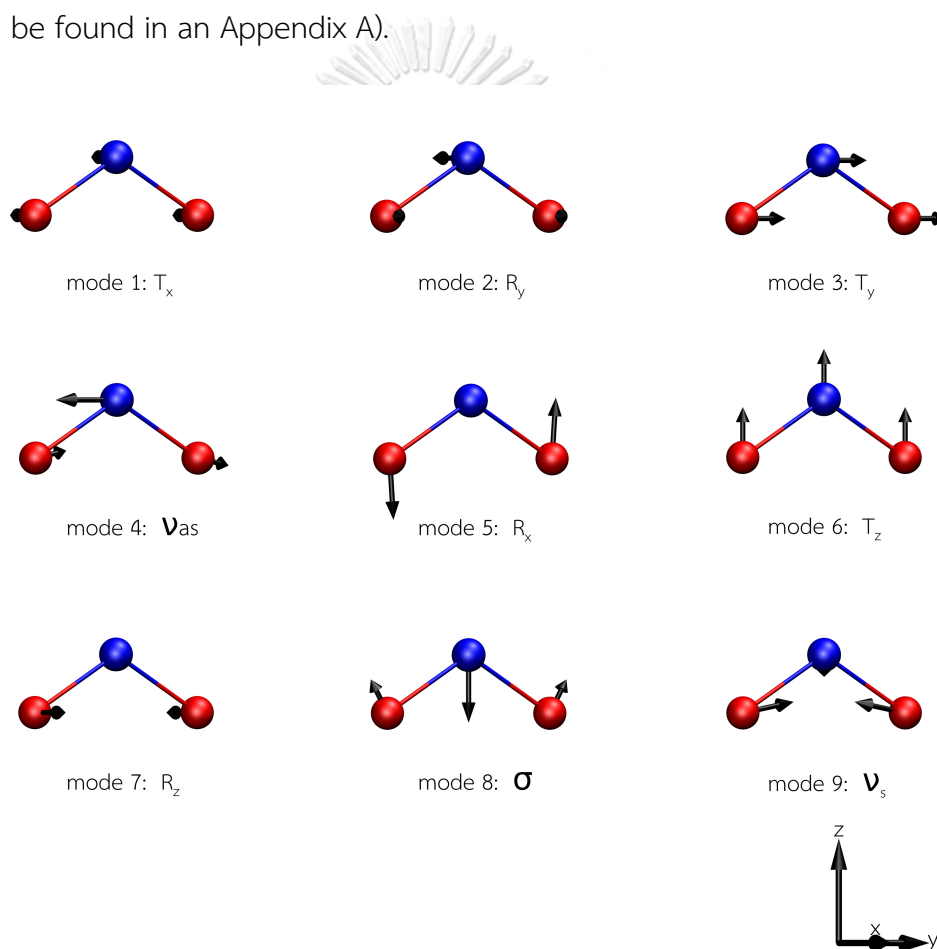

Figure **4.3**: Twelve normal coordinates of an NO_3^- molecule that could be identified as following modes, T_q represents translation in the q-direction, R_q represents rotation around the q-axis, v_q is the qth vibration modes

In the case of the NO_3^- anion, there are a total of 12 modes of motions, including three translation, three rotation, and six vibration modes. The sets of normal coordinates in Figure **4.3** could be explained as translation in the z-axis, translation in the x-axis, in-plane deformation, in-plane deformation, translation in the y-axis, out-of-plane deformation, rotation around the x-axis, anti-symmetric stretching, rotation around the z-axis, rotation around x-axis, anti-symmetric stretching and symmetric stretching modes, respectively.

According to the study, it can be summarized that: The EMIT methodology can provide the complete set of normal coordinates for all systems that used as examples in this research. The eigenvalues for translation modes are always positive, and the significant negative eigenvalues may relate to the rotation modes.
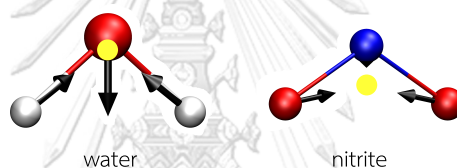
Figure **4.4**: The symmetric stretching modes of a water molecule (left) and a nitrite ion (right). The center of masses is represented in the yellow sphere.

Consider the symmetric stretching modes for the C_{2v} group species in Figure **4.4**. It is well known that the center of mass of NO_2^- is farther from the central atom than in the water molecule. The Figure **4.4** shows that the vectors of the surrounding atoms of NO_2^- deviate from the bonds more than those in the water molecule too. It is the fact that the sets of normal coordinates obtained from the EMIT methodology depend on the center of mass of the molecules, which is not appropriate for the calculation of the power spectra that will be discussed later on.

4.2   A Pseudomolecular Model

So far, it could probably say that EMIT methodology provides a complete set of normal coordinates that resemble those obtained from theory. A pseudomolecular model was introduced and used instead of real molecules to overcome the effect of the center of mass dependent mentioned in the previous section. Figure **4.5** A) shows nine normal coordinates of NO_2^- obtained from EMIT using a pseudomolecular model. The modes could be identified as follow: rotation around the y-axis, translation in the x-direction, translation in the z-direction, bending, symmetric stretching, rotation around the z-axis, anti-symmetric stretching, rotation around the x-axis and translation in the y-direction. Figure **4.5** B) shows the comparison between a symmetric stretching mode and an anti-symmetric stretching mode calculated using an actual molecule and a pseudomolecule. It is seen that, in the case of a pseudomolecular model, the direction of vectors of the surrounding atoms are now almost parallel/anti-parallel to the bonds.

Compare to the Figure **4.2** which is also the NO_2^-. Although the EMIT methodology always provides a complete set of normal coordinates, it is found that the sequence of normal coordinates regarding eigenvalues are different. It has no significance when applying the EMIT methodology to small molecules that easy to display and easy to identify modes pictorially, but it is important for larger molecules that manually identification of modes seems to be impossible. The additional method, thus, to separate the vibration modes of the other motion modes is required.
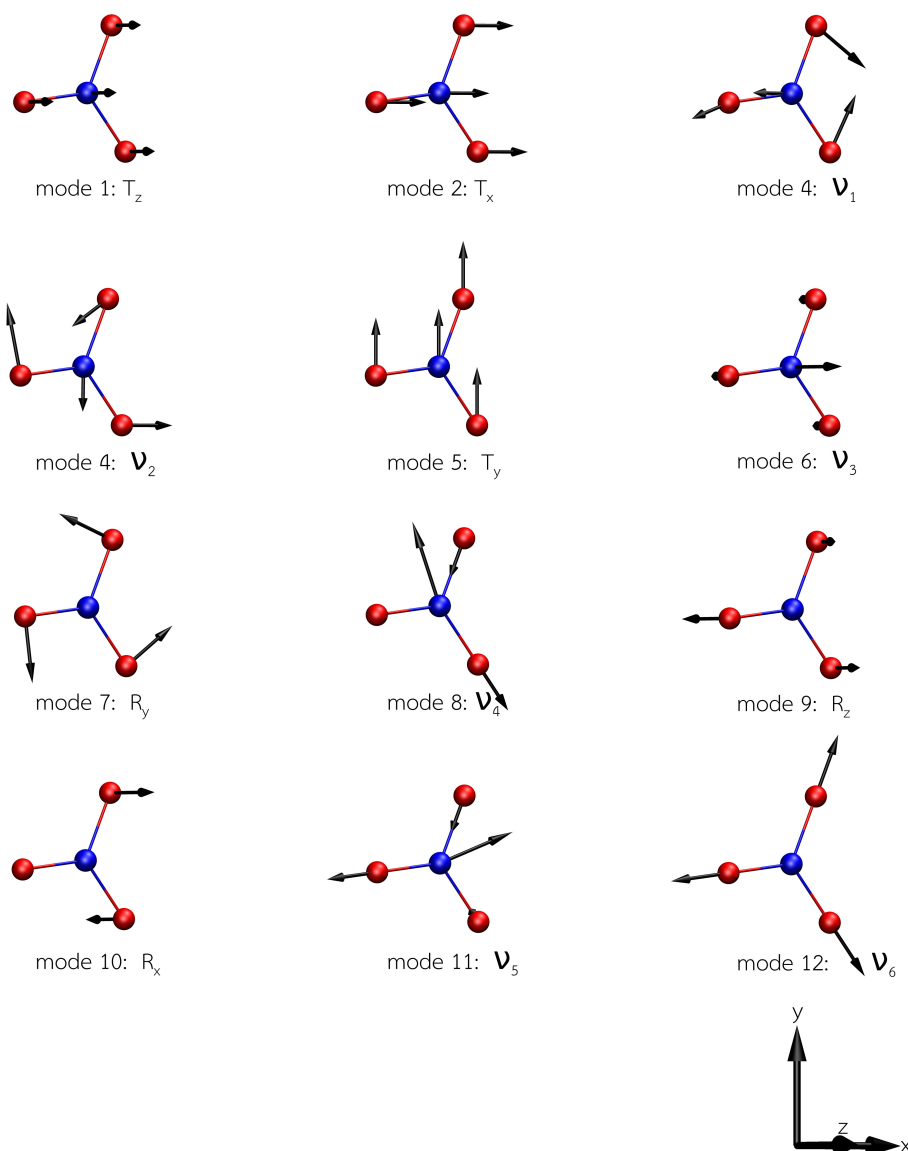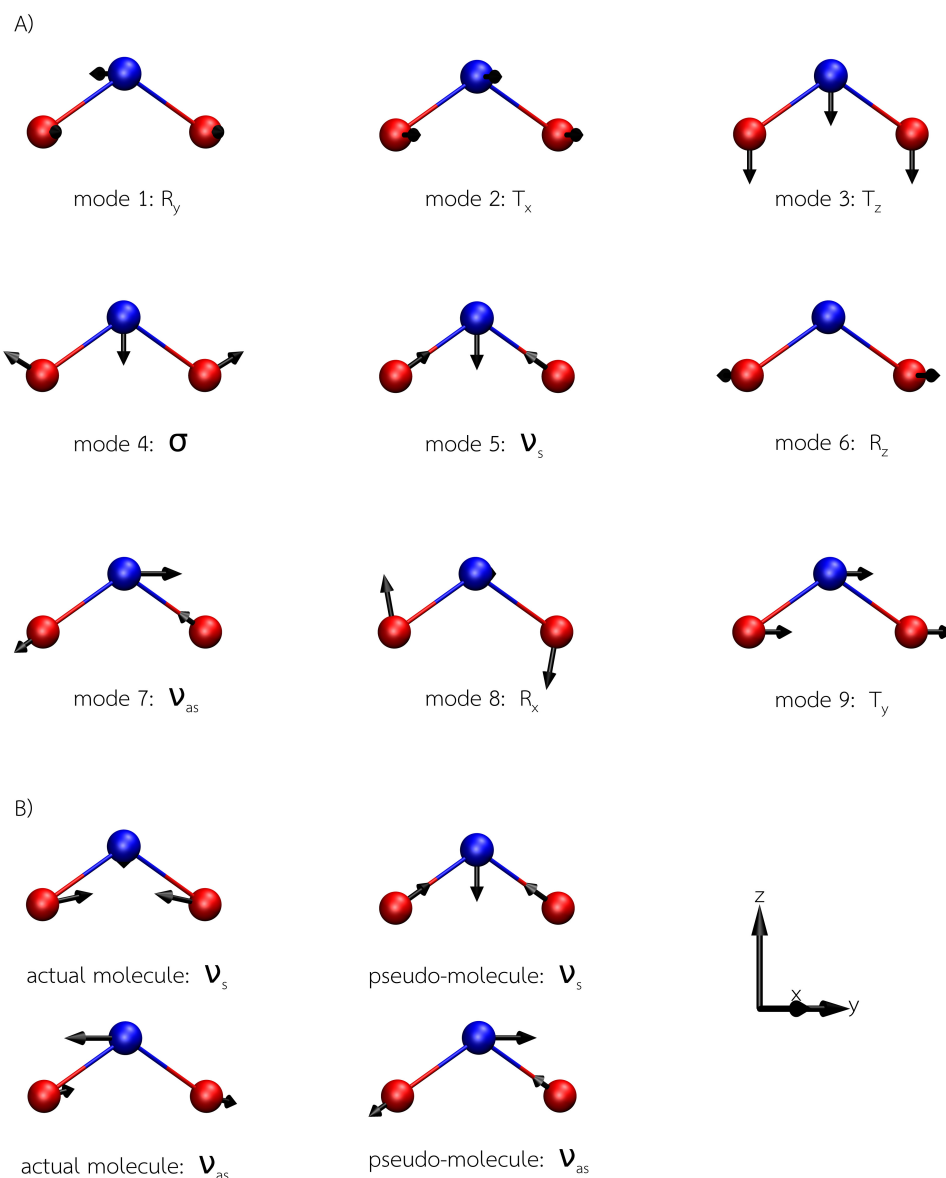
Figure **4.5**: A) Nine normal coordinates of an NO_2^- anion that could be identified as following modes, T_q represents translation in the q-direction, R_q represents rotation around the q-axis, v_s is the symmetric stretching, v_{as} is the anti-symmetric stretching, and σ is the bending modes. B) Comparison between two normal coordinates, symmetric stretching (top) and anti-symmetric stretching (bottom) obtained from an actual molecule (left) and a pseudomolecule (right)

4.3 Separation of Vibration Modes

It is easy to distinguish the vibration modes out of others when the normal coordinates are pictorially represented for some simple molecules, but it is practically impossible for large molecules. Fortunately, there is an approach to construct normal coordinates of translation and rotational modes, as described in Section 2.6.2.

The eigenvalues and corresponding eigenvectors of the water molecule using EMIT with a pseudomolecular model are shown in Table **4.5**.

The translation similarity scoring values of a water molecule are shown in Table **4.6**. According to the score, Column 2, 9, and 3 correspond to translation in the x-, y- and z-direction, respectively. After removing column 2, 9, and 3 out, the remaining columns are shown in Table **4.7**
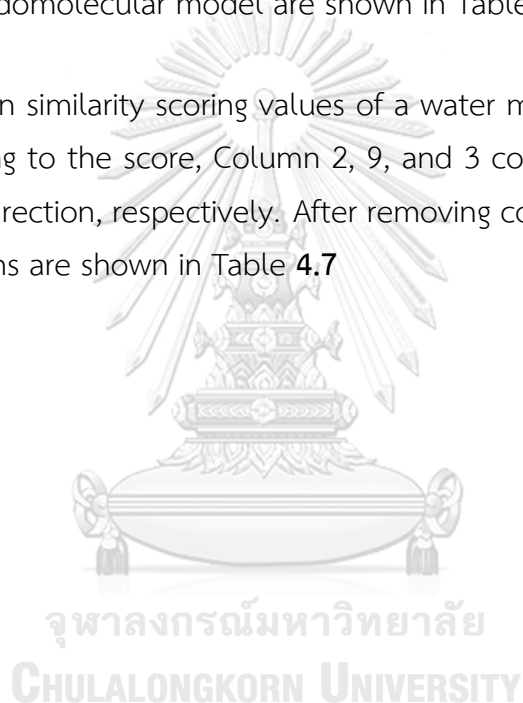
Table **4.5**: The eigenvalues and corresponding eigenvectors of a pseudomolecular model of a water molecule

column	1	2	3	4	5	6	7	8	9
eigenvalues	−0.0003	0.0006	0.0004	−0.0005	0.0000	−0.0009	−0.0007	0.0000	0.0002
eigenvectors	−0.8165	0.5774	0.0000	0.0000	0.0000	0.0000	0.0000	0.0000	0.0000
	0.0000	0.0000	0.0000	0.0000	0.0000	0.0000	−0.3384	−0.7431	0.5774
	0.0000	0.0000	0.5774	0.4823	−0.6589	0.0000	0.0000	0.0000	0.0000
	0.4082	0.5774	0.0000	0.0000	0.0000	−0.7071	0.0000	0.0000	0.0000
	0.0000	0.0000	0.0000	−0.5706	−0.4176	0.0000	0.1692	0.3715	0.5774
	0.0000	0.0000	0.5774	−0.2411	0.3294	0.0000	0.6435	−0.2931	0.0000
	0.4082	0.5774	0.0000	0.0000	0.0000	0.7071	0.0000	0.0000	0.0000
	0.0000	0.0000	0.0000	0.5706	0.4176	0.0000	0.1692	0.3715	0.5774
	0.0000	0.0000	0.5774	−0.2411	0.3294	0.0000	−0.6435	0.2931	0.0000

Table **4.6**: The translation similarity scoring value

column	1	2	3	4	5	6	7	8	9
T_x Score	0.0000	1.0000	0.0000	0.0000	0.0000	0.0000	0.0000	0.0000	0.0000
T_y Score	0.0000	0.0000	0.0000	0.0000	0.0000	0.0000	0.0000	0.0000	1.0000
T_z Score	0.0000	0.0000	1.0000	0.0000	0.0000	0.0000	0.0000	0.0000	0.0000

Table **4.7**: The remaining eigenvalues and corresponding eigenvectors of the water molecule after removing translation modes

column	1	2	3	4	5	6
eigenvalues	−0.0003	−0.0005	0.0000	−0.0009	−0.0007	0.0000
eigenvectors	−0.8165	0.0000	0.0000	0.0000	0.0000	0.0000
	0.0000	0.0000	0.0000	0.0000	−0.3384	−0.7431
	0.0000	0.4823	−0.6589	0.0000	0.0000	0.0000
	0.4082	0.0000	0.0000	−0.7071	0.0000	0.0000
	0.0000	−0.5706	−0.4176	0.0000	0.1692	0.3715
	0.0000	−0.2411	0.3294	0.0000	0.6435	−0.2931
	0.4082	0.0000	0.0000	0.7071	0.0000	0.0000
	0.0000	0.5706	0.4176	0.0000	0.1692	0.3715
	0.0000	−0.2411	0.3294	0.0000	−0.6435	0.2931

The rotation similarity scoring values of a water molecule are shown in Table **4.8**. It is found that columns 5, 1, and 4 in Table **4.7** correspond to rotation around the x-, y- and z-axis, respectively.

Table **4.8**: The rotation similarity scoring value

column	1	2	3	4	5	6
R_x Score	0.0000	0.0000	0.0000	0.0000	0.9566	0.2895
R_y Score	0.9988	0.0000	0.0000	0.0000	0.0000	0.0000
R_z Score	0.0000	0.0000	0.0000	1.0000	0.0000	0.0000

Finally, there are three columns left as the vibration modes, which are shown in Table **4.9**.

Table **4.9**: The remaining eigenvalues and eigenvectors of the water molecule that correspond to vibration modes

column	1	2	3
eigenvalues	−0.0005	0.0000	0.0000
eigenvectors	0.0000	0.0000	0.0000
	0.0000	0.0000	−0.7431
	0.4823	−0.6589	0.0000
	0.0000	0.0000	0.0000
	−0.5706	−0.4176	0.3715
	−0.2411	0.3294	−0.2931
	0.0000	0.0000	0.0000
	0.5706	0.4176	0.3715
	−0.2411	0.3294	0.2931

จุฬาลงกรณ์มหาวิทยาลัย
CHULALONGKORN UNIVERSITY
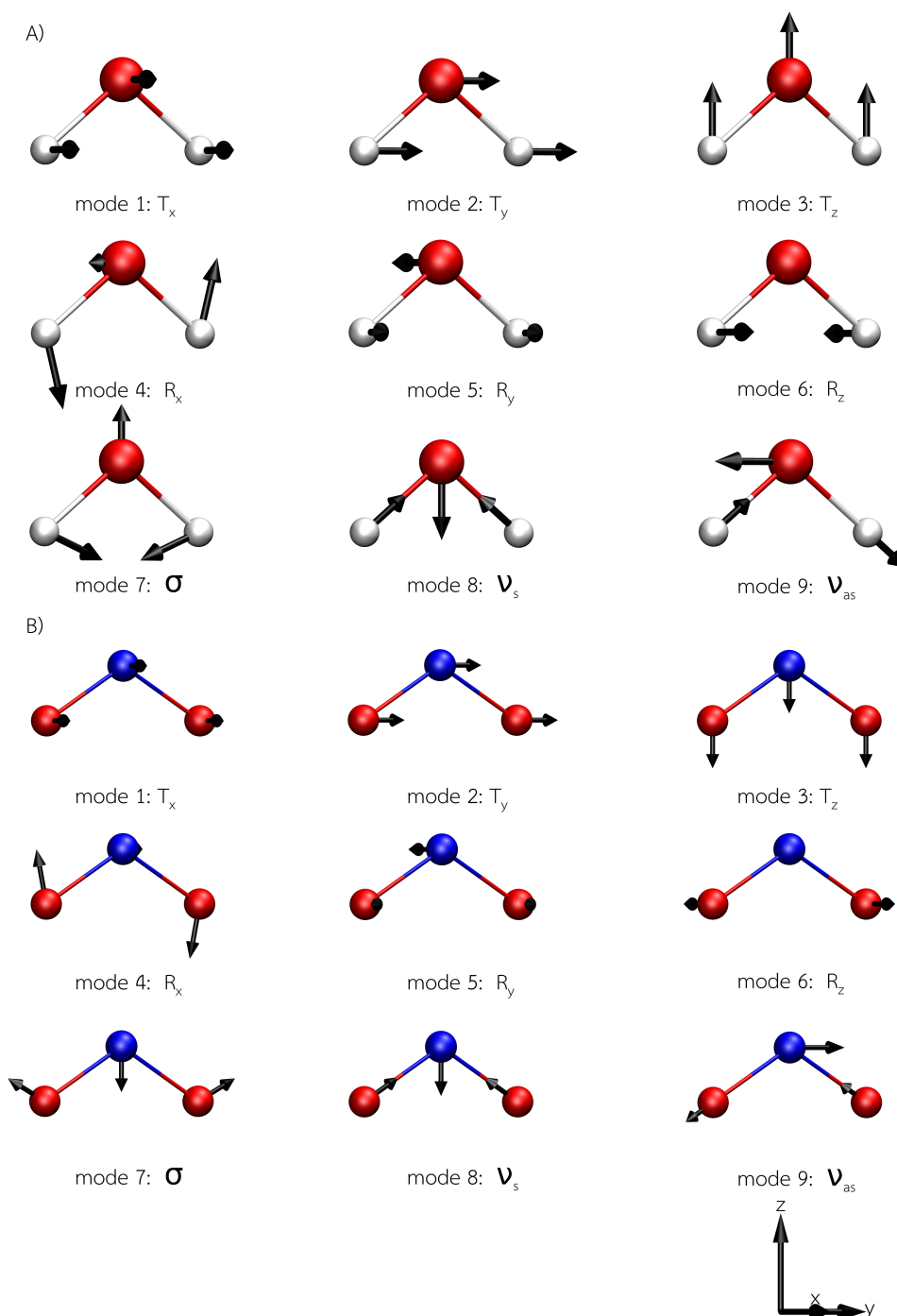
Figure **4.6**: Nine normal coordinates of A) a water molecule and B) a NO$_2^-$ ion after reordering the sequence of modes using the scoring function. The last three modes are assigned as vibration modes.

The ordered normal coordinates of a water molecule, a nitrite ion, and a nitrate

ion are displayed in Figure **4.6** and Figure **4.7**, respectively. According to Figure **4.6** A, B, nine normal coordinates are now shown in the sequence as follows. The first three modes are translation in the x-direction, y-direction, and z-direction, respectively. Moreover, the following three modes are rotation around x-axis, y-axis, and z-axis, respectively. For water, the last three vibration modes are classified as a bending mode, a symmetric stretching mode, and an anti-symmetric stretching mode. For NO_2^-, the last three vibration modes are classified as a bending mode, a symmetric stretching mode, and an anti-symmetric stretching mode. It is evident that for N atoms of non-linear molecules, the last $3N-6$ modes are undoubtedly vibration modes.

Like two previous examples, In the case of NO_3^- shown in Figure **4.7**, the first six modes are three translations and three rotations modes and the last 6 $(3N-6)$ are now vibration modes. On the other hand, the first six modes could be identified as non-vibration modes.

จุฬาลงกรณ์มหาวิทยาลัย
CHULALONGKORN UNIVERSITY
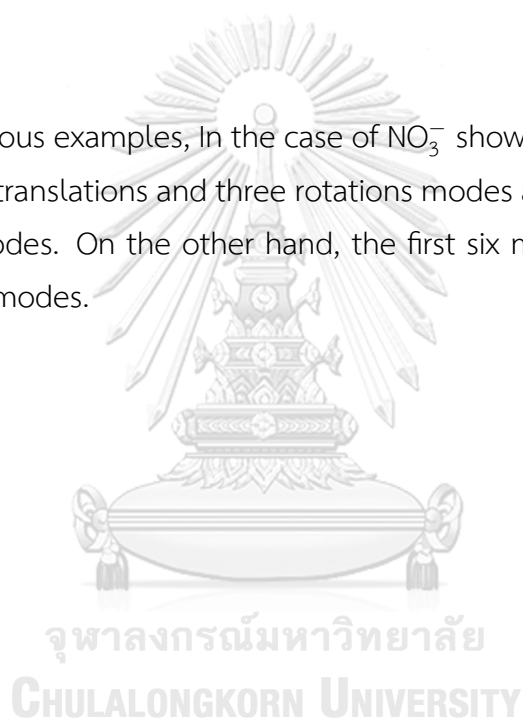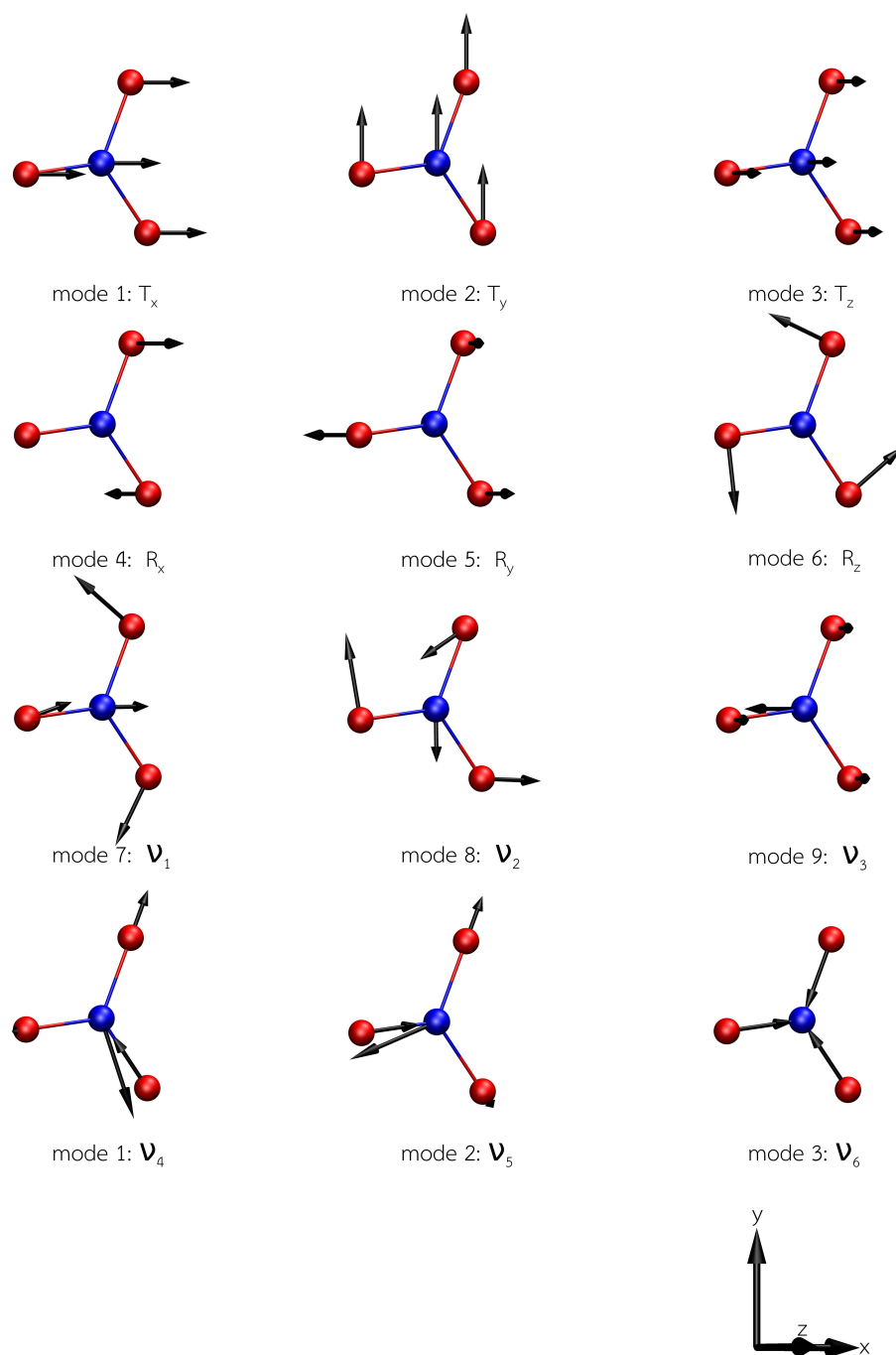
Figure **4.7**: Twelve normal coordinates of a NO_3^- anion after reordering the sequence of modes using the scoring function. The last six modes are assigned as vibration modes.

Table **4.10** shows scalar products representing similarity scores between vibra-

tion mode of Hessian normal coordinates and EMIT normal coordinates. The Hessian normal coordinates are extracted from the frequency calculation of the three systems. In case of H_2O, the values are higher than 0.7 for both EMIT with/without applying pseudomolecule. For NO_2^-, without pseudomolecule the values are about 0.7, meanwhile the values are increased to about 0.9 with pseudomolecule. These results show an important of the pseudomolecule that helps EMIT methodology to provide a set of normal coordinates that are getting closer to the Hessian normal coordinates. In case of NO_3^- that the center of mass is located at the central N atom, the values are above 0.9 for both cases. In summary, the EMIT normal coordinates conform with the Hessian normal coordinates and the pseudomolecule model is important for structures that its center-of-mass shifts from the central atom as seen in NO_2^- meanwhile it does not reduce the similarity when applying to the structure that the center-of-mass is already located at the central atom as in NO_3^-.

Table **4.10**: The absolute values of the scalar products representing similarity of the EMIT normal coordinates and the Hessian normal coordinates*

System	vibration modes[a]		
	σ	ν_{as}	ν_s
H_2O w/o PMM	0.7989	0.7133	0.8074
H_2O w PMM	0.7973	0.7195	0.7832
NO_2^- w/o PMM	0.7766	0.9795	0.7498
NO_2^- w PMM	0.9841	0.9980	0.9754

System	vibration modes[b]					
	ν_1	ν_2	ν_3	ν_4	ν_5	ν_6
NO_3^- w/o PMM	0.9926	0.9926	0.9984	1.0000	0.9145	0.9145
NO_3^- w PMM	0.9926	0.9926	0.9984	1.0000	0.9144	0.9144

[*] w/o PMM and w PMM stand for without pseudomolecule model and with pseudomolecule model, respectively.

[a] σ, ν_{as}, and ν_s are bending, antisymmetric stretching and symmetric stretching modes, respectively.

[b] ν_1 and ν_2 are in-plane deformation modes, ν_3 is the out of plane deformation mode, ν_4 is the symmetric stretching mode, and ν_5 and ν_6 are antisymmetric stretching modes.

4.4   The Power Spectra and the EMIT Methodology

Usually, the traditional theoretical way to calculate spectra of molecules must rely on the quantum mechanical calculation by using the harmonic approximation. However, there is an alternative approach to compute the frequency of the oscillating object by using the Fourier transform (FT) of the auto-correlation function. In computational chemistry, a set of normal coordinates and velocity trajectory can be used for calculation of velocity autocorrelation function (VACF), and VACF will be Fourier transformed into frequency domain that correspond to each mode in normal coordinates.

The vibration power spectrum of NO_2^- and NO_3^- using the EMIT methodology without the pseudomolecular model to compute normal coordinates will be firstly discussed here.

จุฬาลงกรณ์มหาวิทยาลัย
CHULALONGKORN UNIVERSITY
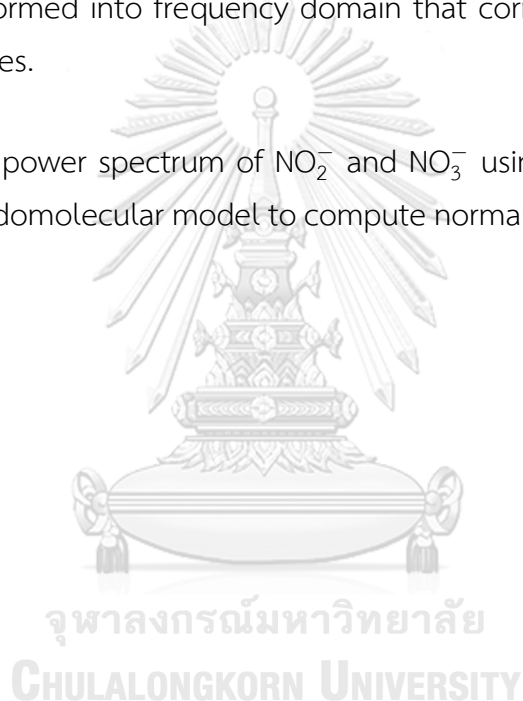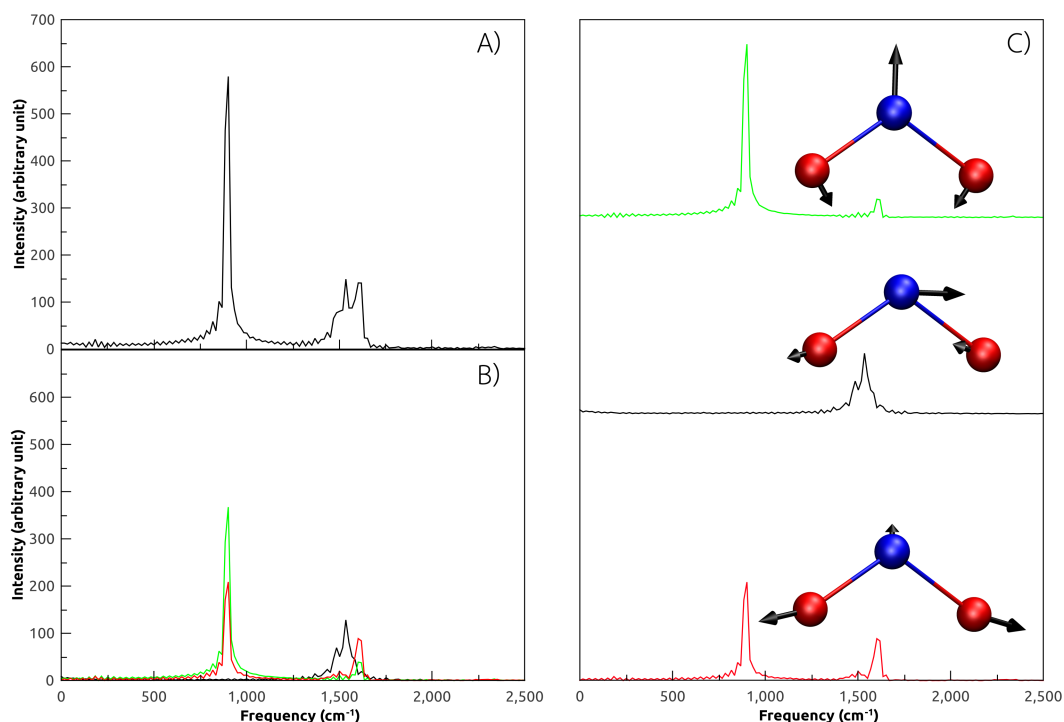
Figure **4.8**: Power spectra of a nitrite ion (NO_2^-) A) Accumulative power spectrum. B) Power spectra for the bending mode (green), anti-symmetric stretching mode (black), and symmetric stretching mode (red). C) Power spectra with corresponding modes for the bending mode (green), anti-symmetric stretching mode (black), and symmetric stretching mode (red).

In the case of NO_2^- in (Figure **4.8** A), it is found that there are three major characteristic peaks at 901, 1535, and 1602 cm^{-1}. However, when represented in an individual spectrum (Figure **4.8** B and C), there are two peaks at 901 and 1602 cm^{-1} for a symmetric stretching mode, there is one peak at 1535 cm^{-1} for an anti-symmetric stretching mode, there are also two peaks at 901 and 1602 cm^{-1} for a bending mode. Please note that two peaks of a symmetric stretching and a bending mode have similar positions, and the highest peak of two modes appears at 901 cm^{-1}, which is unsatisfying for a symmetric stretching that the highest peak should appear at the higher frequency. However, when considering the irreducible representations of vibrations (Γ_{vib}) of the C_{2V} group that is:

$$\Gamma_{vib} = 2A_1 + B_2. \tag{4.1}$$

The vibration modes are identified as A_1 (bending), B_1 (anti-symmetric stretching) and A_1 (symmetric stretching), respectively. Two peaks at 901 and 1602 cm^{-1} come from modes that belong in the same representation, which is acceptable. One mode per peak is still more preferable.
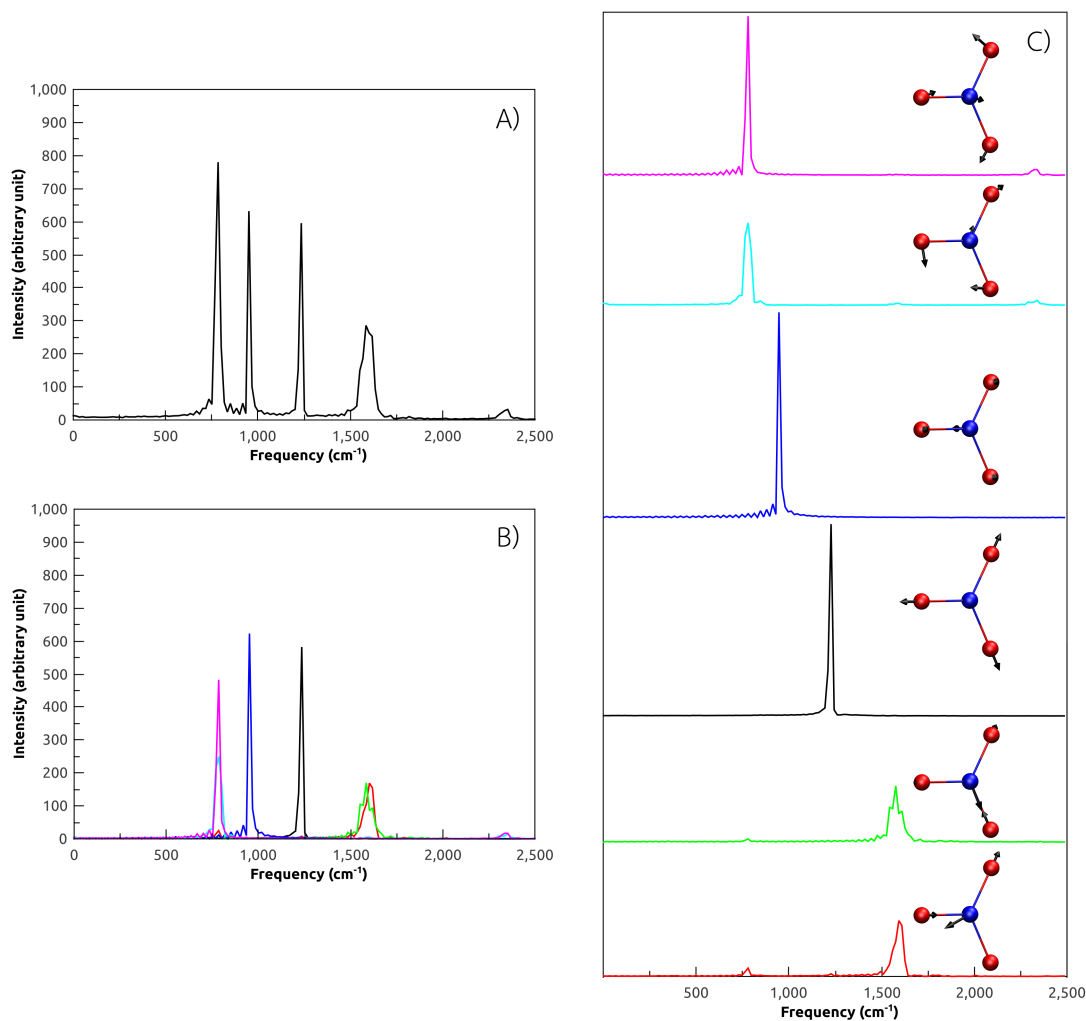
Figure **4.9**: Power spectra of a nitrite anion (NO$_3^-$) A) Accumulative power spectrum. B) Power spectra for the in-plane deformation (ν_1/ν_2, magenta/cyan), out-of-plane deformation (ν_3, blue), symmetric stretching (ν_6, black), and anti-symmetric stretching (ν_4/ν_5, green/red) modes. C) Power spectra with corresponding modes for the in-plane deformation (ν_1/ν_2, magenta/cyan), out-of-plane deformation (ν_3, blue), symmetric stretching (ν_6, black) and anti-symmetric stretching (ν_4/ν_5, green/red) modes.

When represented in one spectrum in (Figure **4.9** A), there are four major characteristic peaks at 784, 951, 1235 and 1585 cm^{-1} for NO$_3^-$. Considering the irreducible representations of vibrations (Γ_{vib}) of the C$_{3V}$ group that is:

$$\Gamma_{vib} = A_1 + A_2 + 2E \tag{4.2}$$

Since there are six vibratoinal modes for NO$_3^-$, there must have two other degeneracy frequencies. In case of an individual spectra shown in Figure **4.9** B and C, there is one doubly degeneracy modes at 784 cm^{-1} which represents two in-plane deformation modes E (ν_1 and ν_2), the peak at 951 cm^{-1} represents the out-of-plane deformation mode A_2, the peak at 1235 cm^{-1} represents the symmetric stretching mode A_1 and two peaks at 1585 and 1602 cm^{-1} stand for the two anti-symmetric stretching modes, these two last peaks are identified as another degeneracy mode E'.

4.5 The Power Spectra and the Role of the Pseudomolecular Model

In the previous section, it is manifest that normal coordinates obtained from the EMIT methodology able to provide the power spectra of the two example anions. Even though there are some degeneracy peaks occur.

Figure **4.10**: Using the EMIT methodology with the pseudomolecular model: Power spectrum of a nitrite anion (NO_2^-) A) Accumulative power spectra. B) Power spectra for the bending mode (green), anti-symmetric stretching mode (black), and symmetric stretching mode (red). C) Power spectra with corresponding modes for the bending mode (green), anti-symmetric stretching mode (black), and symmetric stretching mode (red).

Using the EMIT methodology together with the pseudomolecular model (Figure **4.10**), it is found that in case of NO_2^-, there are 3 individual characteristic frequencies at 901, 1535 and 1602 cm^{-1}. These peaks are identified as A_1 (bending), B_1 (anti-symmetric stretching) and A_1 (symmetric stretching), respectively.

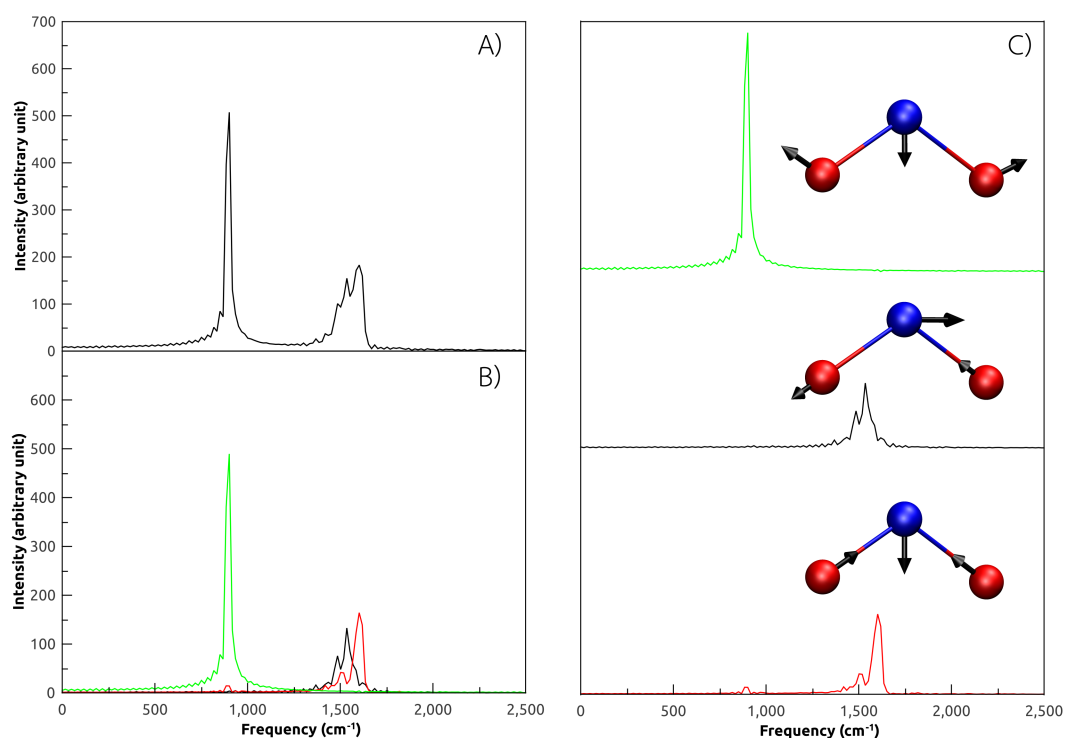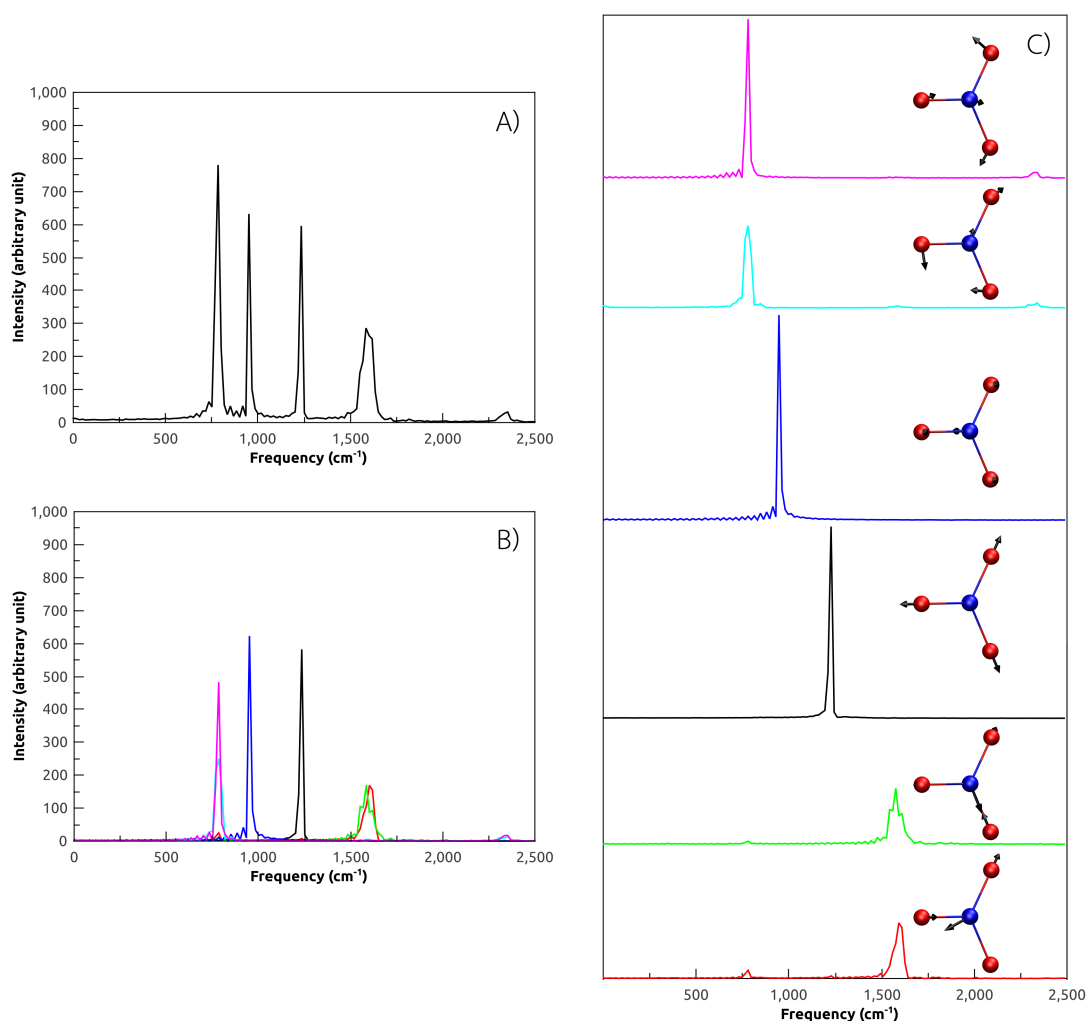Figure **4.11**: Using the EMIT methodology with the pseudomolecular model: Power spectrum of a nitrite ion (NO_3^-) A) Accumulative power spectra. B) Power spectra for the in-plane deformation (ν_1/ν_2, magenta/cyan), out-of-plane deformation (ν_3, blue), symmetric stretching (ν_6, black), and anti-symmetric stretching (ν_4/ν_5, green/red) modes. C) Power spectra with corresponding modes for the in-plane deformation (ν_1/ν_2, magenta/cyan), out-of-plane deformation (ν_3, blue), symmetric stretching (ν_6, black) and anti-symmetric stretching (ν_4/ν_5, green/red) modes.

For NO_3^- in Figure **4.11**, there are 6 characteristic frequencies which can be described as, the in-plane deformation E' (ν_1 and ν_2) modes appeared at 784 cm^{-1}, the A_2 out of plane at 951 cm^{-1}, the A_1 symmetric stretching at 1235 cm^{-1}, and the last two doubly degeneracy, E' appear at 1585 and 1602 cm^{-1}.

It is significantly different between the power spectrum of NO_2^- for EMIT methodology with and without the pseudomolecular model (w-PMM and w/o-PMM, respectively), especially in symmetric stretching and bending mode. Recalling previous Figure **4.8** and Figure **4.10**, in case of w/o-PMM, there are two main peaks at 901 and 1602 cm^{-1} for both symmetric stretching and bending mode which are not seen in case of w/-PMM. Since normal vectors for w/o-PMM are not parallel/anti-parallel to the bond axis, there are some component vectors of bending modes mix with the symmetric stretching mode and vice versa. This deviation is not found in the case of NO_3^-. It is because of the center of mass of NO_3^- is already located near the central N atom even there is no PMM. In contrast, the center of mass of NO_2^- is far away from the central N atom for w/o-PMM but located near the central atom when w/-PMM is applied. These results show the significant role of the PMM that helps to shift the center of mass to the central atom yielding the precise power spectra and, the PMM has not disrupted the molecule that the COM is already located at the central atom. However, the PMM will not necessary if one can develop the EMIT matrix that is independent of the COM.

4.6　Power Spectra Comparison

Comparison with the theoretical calculation and experiments shown in Table **4.11** and **4.12**. It is seen that vibration frequencies obtained from the EMIT methodology w-PMM of NO_2^- and NO_3^- are well agreed with other methods and are slightly larger than the others. The graphs in Figure **4.12** and Figure **4.13** are power spectra obtained from the reference [16, 17] and from this research, respectively. Please note that graphs are resized to let them have the same scale in the frequency axis. According to the graphs, peaks in this research are sharper and clearer, and the position is slightly greater than the reference one. In the case of NO_3^-, the two peaks of anti-symmetric stretching modes are a little splitting, which might be found in the molecular dynamics-based method.

The agreement of power spectra confirms the validity of normal coordinates gained from the EMIT methodology and approves that there is at least one method
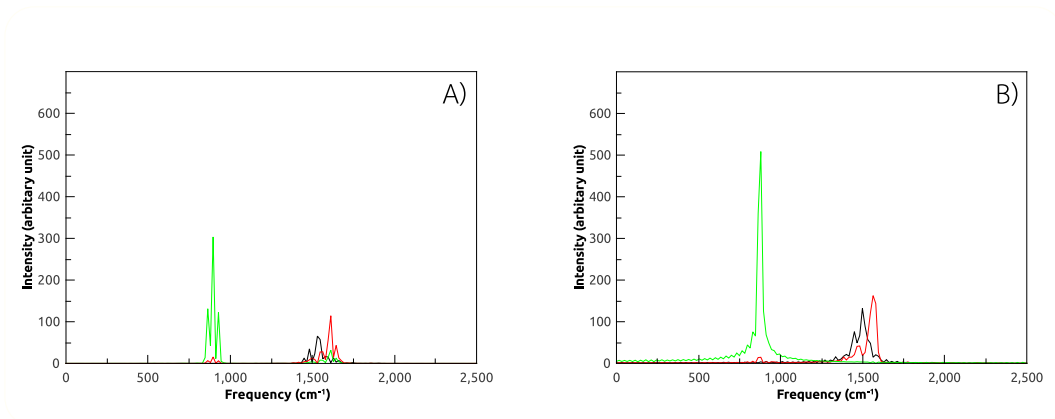
Figure **4.12**: Power spectra of a nitrate anion (NO_2^-) A) obtained from the reference and B) obtained from this research, and the peaks are classified as bending (green), anti-symmetric stretching (black) and symmetric stretching (red)

that able to bypass the construction of the Hessian matrix and using harmonic approximation.

Figure **4.13**: Power spectra of a nitrate anion (NO_3^- A) obtained from the reference and the peaks are classified as the in-plane deformation (ν_1/ν_2, magenta), out-of-plane deformation (ν_3, blue), symmetric stretching (ν_6, black), and anti-symmetric stretching (ν_4/ν_5, red) mod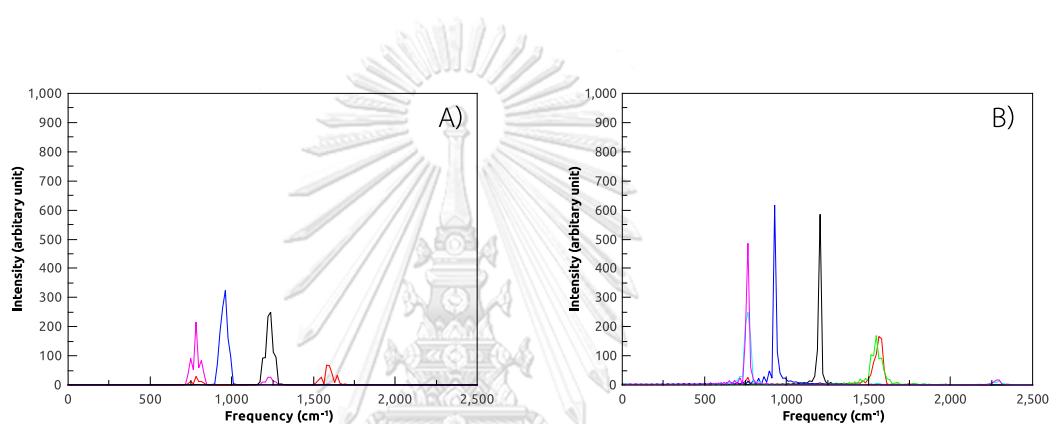es B) Power spectra of a nitrite anion (NO_3^-) obtained from this research and the peaks are classified as the in-plane deformation (ν_1/ν_2, magenta/cyan), out-of-plane deformation (ν_3, blue), symmetric stretching (ν_6, black), and anti-symmetric stretching (ν_4/ν_5, green/red) modes.

Table **4.11**: vibration frequencies (cm^{-1}) of the highest peak for each normal mode of the NO_2^- anion evaluated by the EMIT methodology w-PMM, compared with the experimental data and results calculated at various theoretical levels*

Method	vibration mode of the NO_2^- anion[a]		
	σ	ν_{as}	ν_s
Experimental data			
Solid $NaNO_2$[b]	829	1232	1329
Solid KNO_2[b]	806	1240	1322
$CsNO_2$[b]	803	1230	1317
$Ba(NO_2)_2 \cdot H_2O$[c]	820	1240	1328
Aqueous $NaNO_2$[d]	817	1242	1331
Theoretical results[e]			
HF/6-31G	836[833]	1354[1400]	1449[1446]
MP2/6-31G	733[729]	1340[1370]	1212[1202]
HF/6-31+G(d)	893[889]	1457[1535]	1581[1577]
MP2/6-31+G(d)	789[782]	1352[1395]	1329[1312]
QCISD/6-31+G(d)	791[782]	1235[1288]	1344[1333]
HF/modified-DZ	820[812]	1262[1356]	1458[1418]
MP2/modified-DZ	720[712]	1274[1335]	1201[1185]
HF/DZP+	908[879]	1427[1521]	1635[1584]
MP2/DZP+	823[772]	1310[1363]	1356[1315]
QCISD/DZP+	780[771]	1190[1241]	1346[1334]
G3MP2	896[893]	1527[1579]	1610[1608]
The reference method QMCF MD[f]			
$NO_2^-(H_2O)_{496}$	896[808]	1531[1381]	1612[1454]
EMIT			
$NO_2^-(H_2O)_{496}$	901	1535	1602

[a]σ, ν_{as} and ν_s are bending, anti-symmetric stretching and symmetric stretching modes. [b]Raman data of solid [31]. [c]Raman data of polycrystallineBa$(NO_2)_2 \cdot H_2O$ [32]. [d]Raman data of 5.8 mol dm^{-3} aqueous $NaNO_2$ solution [33]. [e]The values obtained from the optimized geometry with the specified method in the PCM, and the corresponding values for the gas phase presented in square brackets. [f]The values in parentheses were scaled by the factor 0.902 [34]. *Data obtained from the reference [16].

Table **4.12**: vibration frequencies (cm^{-1}) of the highest peak for each normal mode of the NO$_3^-$ anion evaluated by the EMIT methodology w-PMM, compared with the experimental data and results calculated at various theoretical levels

| | vibration mode of the NO$_3^-$ anion[a] | | | |
Method	E'	A_2''	A_1'	E'
Experimental data [35]	718	832	1048	1348
Theoretical results				
MP2	712	790	1070	1529
CCSD	715	821	1088	1440
HF/MM MD	709	712	1088	1401, 1441
B3LYP/MM MD	649	710	965	1237, 1313
The reference QMCF MD method [17]	782	961	1238	1580
EMIT	784	951	1235	1585,1602

[a]E' is the in-plane deformation mode, A_2'' is the out of plane deformation mode, A_1' is symmetric stretching mode and the last E' is the anti-symmetric stretching mode. Data obtained from the reference [17]

CHAPTER V

CONCLUSION

This work shows the success of the Expanded Moment of Inertia Tensor or EMIT methodology in the calculation of a complete set of normal coordinates without either constructing Hessian matrices or using harmonic approximation. Since, mathematically, there are numerous sets of normal coordinates can be obtained for one single molecule, but the set that resembles the group theory analysis is the most preferred. For validation, the calculations of power spectra of two NO_2^- and NO_3^- anions are used as examples, and it turns out that the EMIT methodology provides a set of normal modes that yield good power spectra for the molecule that the center of mass is located at or near the central atom as in NO_3^-. Meanwhile, For molecules like NO_2^- which the center of mass is far away from the central atom, using the pseudomolecular model, the model that allows shifting the center of mass to the central atom, instead of the actual molecules provides a set of normal coordinates that yields the good power spectra. No significant differences of the power spectrum of NO_3^- obtained from with/without using the pseudomolecular model (PMM) confirm that PMM does not affect to those molecules that the center of mass has already located at the central atom. Thus, using EMIT methodology, along with PMM, is recommended for any molecules.

Although two anions had been tested here, this work successfully proved that there is at least one of the non-Hessian based methods which provide a complete set of normal coordinates. On the other hand, this EMIT methodology produces a complete set of normal coordinates from only molecular geometry. Furthermore, the next challenging work is to investigate that the EMIT methodology is capable of calculating normal coordinates for either larger or even macromolecules.

REFERENCES

[1] Belkacem, K., Kupka, F., Samadi, R. and Grimm-Strele, H. Solar p-mode damping rates: Insight from a 3D hydrodynamical simulation. Astronomy & Astrophysics 625 (2019): A20.

[2] Chujo, T., Mori, O. and Kawaguchi, J. Normal mode analysis of rubble-pile asteroids using a discrete element method. Icarus 321 (2019): 458–472.

[3] Woodhouse, J.H. and Deuss, A. 1.03 - Theory and Observations - Earth's Free Oscillations. In G. Schubert (editor), Treatise on Geophysics (Second Edition), pp. 79–115. Oxford: Elsevier, 2015.

[4] Deuss, A., Irving, J.C.E. and Woodhouse, J.H. Regional Variation of Inner Core Anisotropy from Seismic Normal Mode Observations. Science 328(5981) (2010): 1018–1020.

[5] Massarczyk, M., Schlitter, J., Kötting, C., Rudack, T. and Gerwert, K. Monitoring transient events in infrared spectra using local mode analysis. Proteins: Structure, Function, and Bioinformatics 86(10) (2018): 1013–1019.

[6] Henzler-Wildman, K. and Kern, D. Dynamic personalities of proteins. Nature 450 (2007): 964–972.

[7] Bahar, I., Lezon, T.R., Bakan, A. and Shrivastava, I.H. Normal Mode Analysis of Biomolecular Structures: Functional Mechanisms of Membrane Proteins. Chemical Reviews 110(3) (2010): 1463–1497.

[8] Skjaerven, L., Hollup, S.M. and Reuter, N. Normal mode analysis for proteins. Journal of Molecular Structure: THEOCHEM 898(1) (2009): 42–48.

[9] Brünken, S., Sipilä, O., Chambers, E.T., Harju, J., Caselli, P., Asvany, O., Honingh, C.E., Kamiński, T., Menten, K.M., Stutzki, J. and Schlemmer, S. $H2D^+$ observations give an age of at least one million years for a cloud core forming Sun-like stars. Nature 516 (2014): 219–221.

[10] Ogata, H., Nishikawa, K. and Lubitz, W. Hydrogens detected by subatomic resolution protein crystallography in a [NiFe] hydrogenase. Nature 520 (2015): 571–574.

[11] Kato, H.E., Inoue, K., Abe-Yoshizumi, R., Kato, Y., Ono, H., Konno, M., Hososhima, S., Ishizuka, T., Hoque, M.R., Kunitomo, H., Ito, J., Yoshizawa, S., Yamashita, K., Takemoto, M., Nishizawa, T., Taniguchi, R., Kogure, K., Maturana, A.D., Iino, Y., Yawo, H., Ishitani, R., Kandori, H. and Nureki, O. Structural basis for Na^+ transport mechanism by a light-driven Na^+ pump. Nature 521 (2015): 48–53.

[12] Semmlow, J. Chapter 4 - Signal Analysis in the Frequency Domain — Implications and Applications. In J. Semmlow (editor), Circuits, Signals and Systems for Bioengineers (Third Edition), Biomedical Engineering, pp. 169–206. Academic Press, 2018.

[13] Camera, S., Fonseca, J., Maartens, R. and Santos, M.G. Optimized angular power spectra for spectroscopic galaxy surveys. Monthly Notices of the Royal Astronomical Society 481(1) (2018): 1251–1261.

[14] Wilson, M.J., Peacock, J.A., Taylor, A.N. and de la Torre, S. Rapid modelling of the redshift-space power spectrum multipoles for a masked density field. Monthly Notices of the Royal Astronomical Society 464(3) (2017): 3121–3130.

[15] Micarelli, A., Viziano, A., Panella, M., Micarelli, E. and Alessandrini, M. Power spectra prognostic aspects of impulsive eye movement traces in superior vestibular neuritis. Medical & Biological Engineering & Computing 57(8) (2019): 1617–1627.

[16] Vchirawongkwin, S., Kritayakornupong, C., Tongraar, A. and Vchirawongkwin, V. Hydration properties determining the reactivity of nitrite in aqueous solution. Dalton Trans 43 (2014): 12164–12174.

[17] Vchirawongkwin, V., Kritayakornupong, C., Tongraar, A. and Rode, B.M. Symmetry Breaking and Hydration Structure of Carbonate and Nitrate in Aqueous Solutions: A Study by Ab Initio Quantum Mechanical Charge Field Molecular Dynamics. The Journal of Physical Chemistry B 115(43) (2011): 12527–12536.

[18] Humphrey, W., Dalke, A. and Schulten, K. VMD: Visual molecular dynamics. Journal of Molecular Graphics 14(1) (1996): 33–38.

[19] Ochterski, J.W. Vibrational Analysis in Gaussian, 1999. http://gaussian.com/ vib/. [2019, November 27].

[20] Classical Normal Mode Analysis: Harmonic Approximation. http:// www.colby.edu/ chemistry/ PChem/ notes/ NormalModesText.pdf. [2019, November 27].

[21] Kelly, P. 5.3: The Harmonic Oscillator Approximates Vibrations. https:// chem.libretexts.org/ Courses/ Pacific_Union_College/ Quantum_Chemistry/ 05 [2019, November 27].

[22] Fitzpatrick, R. Moment of Inertia Tensor, 2011. http://farside.ph.utexas.edu/ teaching/336k/Newtonhtml/node64.html. [2019, November 27].

[23] Bengtsson, V. and Weisstein, E.W. Diagonalizable Matrix. http:// math-world.wolfram.com/DiagonalizableMatrix.html. [2019, November 27].

[24] Roby, T. 5.3 Diagonalization, 2003. http://www2.math.uconn.edu/ troby/ math2210f16/LT/. [2019, November 27].

[25] Guennebaud, G., Jacob, B. et al. Eigen v3, 2010. http://eigen.tuxfamily.org. [2019, November 27].

[26] Blundell, M. and Harty, D. Chapter 2 - Kinematics and Dynamics of Rigid Bodies. In M. Blundell and D. Harty (editors), The Multibody Systems Approach to Vehicle Dynamics (Second Edition), pp. 27–86. Oxford: Butterworth-Heinemann, 2015.

[27] Bhattacharjee, A., Hofer, T.S., Pribil, A.B., Randolf, B.R., Lim, L.H.V., Lichtenberger, A.F. and Rode, B.M. Revisiting the Hydration of Pb(II): A QMCF MD Approach. The Journal of Physical Chemistry B 113(39) (2009): 13007–13013.

[28] Weisstein, E.W. Fourier Transform. http://mathworld.wolfram.com/Fourier-Transform.html. [2019, November 27].

[29] Weisstein, E.W. Discrete Fourier Transform. http://mathworld.wolfram.com/ DiscreteFourierTransform.html. [2019, November 27].

[30] Roberts, S. Lecture 7 - TheDiscreteFourierTransform. http://www.robots.ox.ac.uk/ sjrob/Teaching/SP/l7.pdf. [2019, November 27].

[31] Brooker, M.H. and Irish, D.E. Infrared and Raman Spectroscopic Studies of Solid Alkali Metal Nitrites. Canadian Journal of Chemistry 49(8) (1971): 1289–1295.

[32] Lamba, O. and Bist, H. Infrared and raman spectra of barium nitrite monohydrate. Journal of Physics and Chemistry of Solids 44(5) (1983): 445–452.

[33] Irish, D.E. and Thorpe, R.V. Raman Spectral Studies of Cadmium–Nitrite Interactions in Aqueous Solutions and Crystals. Canadian Journal of Chemistry 53(10) (1975): 1414–1423.

[34] Vchirawongkwin, V. and Rode, B.M. Solvation energy and vibrational spectrum of sulfate in water – An ab initio quantum mechanical simulation. Chemical Physics Letters 443(1) (2007): 152–157.

[35] Rudolph, W.W., Fischer, D. and Irmer, G. "Vibrational Spectroscopic Studies and Density Functional Theory Calculations of Speciation in the CO_2—Water System". Applied Spectroscopy 60(2) (2006): 130–144.

APPENDICES

APPENDIX A

OUTPUT

A.1   Output for NO_2^-

Table A.1: Coordinates of NO_2^- in Angstrom after energy optimization.

Atom	x	y	z
N	0.0000	0.0000	0.4640
O1	0.0000	1.0741	−0.2030
O2	0.0000	−1.0741	−0.2030

Table A.2: An AMIT of each atom in NO_2^-

Atom	AMIT		
N	3.0142	0.0000	0.0000
	0.0000	3.0142	0.0000
	0.0000	0.0000	0.0000
O1	19.1189	0.0000	0.0000
	0.0000	0.6597	3.4896
	0.0000	3.4896	18.4592
O2	19.1189	0.0000	0.0000
	0.0000	0.6597	−3.4896
	0.0000	−3.4896	18.4592

Table A.3: The EMIT matrix of NO_2^-

−1.0047	0.0000	0.0000	7.3777	0.0000	0.0000	7.3777	0.0000	0.0000
0.0000	−1.0047	0.0000	0.0000	1.2246	1.1632	0.0000	1.2246	−1.1632
0.0000	0.0000	0.0000	0.0000	1.1632	6.1531	0.0000	−1.1632	6.1531
7.3777	0.0000	0.0000	−6.3730	0.0000	0.0000	12.7459	0.0000	0.0000
0.0000	1.2246	1.1632	0.0000	−0.2199	−1.1632	0.0000	0.4398	0.0000
0.0000	1.1632	6.1531	0.0000	−1.1632	−6.1531	0.0000	0.0000	12.3062
7.3777	0.0000	0.0000	12.7459	0.0000	0.0000	−6.3730	0.0000	0.0000
0.0000	1.2246	−1.1632	0.0000	0.4398	0.0000	0.0000	−0.2199	1.1632
0.0000	−1.1632	6.1531	0.0000	0.0000	12.3062	0.0000	1.1632	−6.1531

Table A.4: The eigenvalues and corresponding eigenvectors of NO$_2^-$

column	1	2	3	4	5	6	7	8	9
eigenvalues	13.7507	−8.3824	1.4445	−1.9830	−18.7056	12.3062	−19.1189	−6.8128	0.0000
eigenvectors	−0.5774	−0.8165	0.0000	0.0000	0.0000	0.0000	0.0000	0.0000	0.0000
	0.0000	0.0000	0.5774	−0.8105	−0.0991	0.0000	0.0000	0.0000	0.0000
	0.0000	0.0000	0.0000	0.0000	0.0000	0.5774	0.0000	−0.7760	−0.2541
	−0.5774	0.4082	0.0000	0.0000	0.0000	0.0000	−0.7071	0.0000	0.0000
	0.0000	0.0000	0.5774	0.4052	0.0496	0.0000	0.0000	0.2200	−0.6720
	0.0000	0.0000	0.0000	−0.0858	0.7019	0.5774	0.0000	0.3880	0.1270
	−0.5774	0.4082	0.0000	0.0000	0.0000	0.0000	0.7071	0.0000	0.0000
	0.0000	0.0000	0.5774	0.4052	0.0496	0.0000	0.0000	−0.2200	0.6720
	0.0000	0.0000	0.0000	0.0858	−0.7019	0.5774	0.0000	0.3880	0.1270

A.2   Output for NO_3^-

Table A.5: Coordinates of NO_3^- in Angstrom after energy optimization.

Atom	x	y	z
N	−0.0002	−0.0001	0.0000
O1	0.7640	−1.0037	0.0000
O2	0.4877	1.1632	0.0000
O3	−1.2516	−0.1594	0.0000

Table A.6: An AMIT of each atom in NO_3^-

Atom	AMIT		
N	0.0000	0.0000	0.0000
	0.0000	0.0000	0.0000
	0.0000	0.0000	0.0000
O1	16.1179	12.2689	0.0000
	12.2689	9.3390	−0.0001
	0.0000	−0.0001	25.4569
O2	21.6461	−9.0767	0.0000
	−9.0767	3.8061	0.0001
	0.0000	0.0001	25.4522
O3	0.4066	−3.1922	−0.0001
	−3.1922	25.0637	0.0000
	−0.0001	0.0000	25.4703

Table A.7: The EMIT matrix of NO_3^-

0.0000	0.0000	0.0000	4.0295	3.0672	0.0000	5.4115	-2.2692	0.0000	0.1016	-0.7981	0.0000
0.0000	0.0000	0.0000	3.0672	2.3348	0.0000	-2.2692	0.9515	0.0000	-0.7981	6.2659	0.0000
4.0295	3.0672	0.0000	-8.0590	-6.1344	0.0000	9.4410	0.7981	0.0000	4.1311	2.2692	0.0000
3.0672	2.3348	0.0000	-6.1344	-4.6695	0.0000	0.7981	3.2863	0.0000	2.2692	8.6007	0.0000
0.0000	0.0000	6.3642	0.0000	0.0000	-12.7285	0.0000	0.0000	12.7273	0.0000	0.0000	12.7318
5.4115	-2.2692	0.0000	9.4410	0.7981	0.0000	-10.8231	4.5383	0.0000	5.5132	-3.0672	0.0000
-2.2692	0.9515	0.0000	0.7981	3.2863	0.0000	4.5383	-1.9030	0.0000	-3.0672	7.2174	0.0000
0.0000	0.0000	6.3630	0.0000	0.0000	12.7273	0.0000	0.0000	-12.7261	0.0000	0.0000	12.7306
0.1016	-0.7981	0.0000	4.1311	2.2692	0.0000	5.5132	-3.0672	0.0000	-0.2033	1.5961	0.0000
-0.7981	6.2659	0.0000	2.2692	8.6007	0.0000	-3.0672	7.2174	0.0000	1.5961	-12.5319	0.0000
0.0000	0.0000	6.3676	0.0000	0.0000	12.7318	0.0000	0.0000	12.7306	0.0000	0.0000	-12.7351

Table A.8: The eigenvalues and corresponding eigenvectors of NO_3^-

column	1	2	3	4	5	6	7	8	9	10	11	12
eigenvalues	19.0949	9.5427	−15.9117	−15.9130	9.5522	−6.3649	−25.4598	0.0000	−25.4652	−25.4544	0.0000	0.0000
eigenvectors	0.0000	0.5000	−0.3872	−0.0067	0.0000	0.0000	−0.0001	−0.2723	0.0000	0.0000	0.7252	−0.0001
	0.0000	0.0000	0.0067	−0.3873	0.5000	0.0000	0.0002	0.7251	0.0000	0.0000	0.2723	0.0000
	0.5000	0.0000	0.0000	0.0000	0.0000	0.8660	0.0000	0.0000	0.0002	0.0001	0.0000	0.0000
	0.0000	0.5000	0.2580	0.5025	0.0000	0.0000	0.4591	0.2996	0.0000	0.0000	−0.0898	0.3497
	0.0000	0.0000	0.4978	0.0002	0.5000	0.0000	0.3498	−0.3936	0.0000	0.0000	0.1179	−0.4594
	0.5000	0.0000	0.0000	0.0000	0.0000	−0.2887	0.0000	0.0000	0.4955	−0.6489	0.0000	0.0000
	0.0000	0.5000	0.4976	−0.3601	0.5000	0.0000	−0.5320	−0.1453	0.0000	0.0000	−0.1370	0.2232
	0.0000	0.0000	−0.3643	−0.2391	0.0000	0.0000	0.2233	−0.3465	0.0000	0.0000	−0.3267	0.5324
	0.5000	0.0000	0.0000	0.0000	0.0000	−0.2888	0.0000	0.0000	0.3142	0.7536	0.0000	0.0000
	0.0000	0.5000	−0.3685	−0.1357	0.5000	0.0000	0.0730	0.1180	0.0000	0.0000	−0.4984	−0.5728
	0.0000	0.0000	−0.1401	0.6262	0.0000	0.0000	−0.5733	0.0150	0.0000	0.0000	−0.0635	−0.0730
	0.5000	0.0000	0.0000	0.0000	0.0000	−0.2885	0.0000	0.0000	−0.8098	−0.1047	0.0000	0.0000

A.3 Reordering modes for NO_2^-

Table A.9: The eigenvalues and corresponding eigenvectors of a pseudo-molecular model of NO_2^-

column	1	2	3	4	5	6	7	8	9
eigenvalues	0.0005	0.0011	0.0008	−0.0008	0.0000	−0.0016	0.0000	−0.0013	0.0003
eigenvectors	−0.8165	0.5774	0.0000	0.0000	0.0000	0.0000	0.0000	0.0000	0.0000
	0.0000	0.0000	0.0000	0.0000	0.0000	0.0000	0.7686	0.2755	0.5774
	0.0000	0.0000	−0.5774	−0.5560	−0.5979	0.0000	0.0000	0.0000	0.0000
	0.4082	0.5774	0.0000	0.0000	0.0000	0.7071	0.0000	0.0000	0.0000
	0.0000	0.0000	0.0000	0.5178	−0.4815	0.0000	−0.3843	−0.1378	0.5774
	0.4082	0.5774	−0.5774	0.2780	0.2990	0.0000	0.2386	−0.6656	0.0000
	0.0000	0.0000	0.0000	0.0000	0.0000	−0.7071	0.0000	0.0000	0.0000
	0.0000	0.0000	0.0000	−0.5178	0.4815	0.0000	−0.3843	−0.1378	0.5774
	0.0000	0.0000	−0.5774	0.2780	0.2990	0.0000	−0.2386	0.6656	0.0000

Table A.10: The translation similarity scoring values of NO_2^-

column	1	2	3	4	5	6	7	8	9
T_x Score	0.0000	1.0000	0.0000	0.0000	0.0000	0.0000	0.0000	0.0000	0.0000
T_y Score	0.0000	0.0000	0.0000	0.0000	0.0000	0.0000	0.0000	0.0000	1.0000
T_z Score	0.0000	0.0000	1.0000	0.0000	0.0000	0.0000	0.0000	0.0000	0.0000

Table A.11: The remaining eigenvalues and corresponding eigenvectors of NO_2^- after removing translation modes

column	1	2	3	4	5	6
eigenvalues	0.0005	−0.0008	0.0000	−0.0016	0.0000	−0.0013
eigenvectors	−0.8165	0.0000	0.0000	0.0000	0.0000	0.0000
	0.0000	0.0000	0.0000	0.0000	0.7686	0.2755
	0.0000	−0.5560	−0.5979	0.0000	0.0000	0.0000
	0.4082	0.0000	0.0000	0.7071	0.0000	0.0000
	0.0000	0.5178	−0.4815	0.0000	−0.3843	−0.1378
	0.0000	0.2780	0.2990	0.0000	0.2386	−0.6656
	0.4082	0.0000	0.0000	−0.7071	0.0000	0.0000
	0.0000	−0.5178	0.4815	0.0000	−0.3843	−0.1378
	0.0000	0.2780	0.2990	0.0000	−0.2386	0.6656

Table A.12: The rotation similarity scoring values of NO_2^-

column	1	2	3	4	5	6
R_x Score	0.0000	0.0000	0.0000	0.0000	0.0257	0.8933
R_y Score	0.5256	0.0000	0.0000	0.0000	0.0000	0.0000
R_z Score	0.0000	0.0000	0.0000	1.0000	0.0000	0.0000

Table A.13: The remaining eigenvalues and eigenvectors of NO_2^- that correspond to vibration modes

column	1	2	3
eigenvalues	−0.0008	0.0000	0.0000
eigenvectors	0.0000	0.0000	0.0000
	0.0000	0.0000	0.7686
	−0.5560	−0.5979	0.0000
	0.0000	0.0000	0.0000
	0.5178	−0.4815	−0.3843
	0.2780	0.2990	0.2386
	0.0000	0.0000	0.0000
	−0.5178	0.4815	−0.3843
	0.2780	0.2990	−0.2386

A.4 Reordering modes for NO_3^-

Table A.14: The eigenvalues and corresponding eigenvectors of a pseudo-molecular model of NO_3^-

column	1	2	3	4	5	6	7	8	9	10	11	12
eigenvalues	0.0012	0.0006	−0.0010	−0.0010	0.0006	−0.0004	−0.0016	−0.0016	−0.0016	0.0000	0.0000	0.0000
eigenvectors	0.0000	0.5000	0.3871	0.0067	0.0000	0.0000	0.0000	0.0000	0.0000	0.2723	−0.7252	−0.0005
	0.0000	0.0000	0.0068	−0.3874	0.5000	0.0000	0.0001	0.0000	0.0000	−0.7251	−0.2723	−0.0002
	0.5000	0.0000	0.0000	0.0000	0.0000	−0.8660	0.0000	0.0001	0.0000	0.0000	0.0000	0.0000
	0.0000	0.5000	−0.2753	0.4931	0.0000	0.0000	0.4592	0.0000	0.0000	−0.2997	0.0896	−0.3497
	0.0000	0.0000	−0.4976	−0.0170	0.5000	0.0000	0.3498	0.0000	0.0000	0.3936	−0.1177	0.4592
	0.5000	0.0000	0.0000	0.0000	0.0000	0.2887	0.0000	0.5072	−0.6398	0.0000	0.0000	0.0000
	0.0000	0.5000	−0.4847	−0.3770	0.0000	0.0000	−0.5321	0.0000	0.0000	0.1453	0.1369	−0.2231
	0.0000	0.0000	0.3724	0.2264	0.5000	0.0000	0.2233	0.0000	0.0000	0.3465	0.3265	−0.5320
	0.5000	0.0000	0.0000	0.0000	0.0000	0.2887	0.0000	0.3005	0.7592	0.0000	0.0000	0.0000
	0.0000	0.5000	0.3729	−0.1229	0.0000	0.0000	0.0729	0.0000	0.0000	−0.1180	0.4987	0.5733
	0.0000	0.0000	0.1184	0.6308	0.5000	0.0000	−0.5731	0.0000	0.0000	−0.0150	0.0635	0.0730
	0.5000	0.0000	0.0000	0.0000	0.0000	0.2886	0.0000	−0.8077	−0.1194	0.0000	0.0000	0.0000

Table A.15: The translation similarity scoring values of NO_3^-

column	1	2	3	4	5	6	7	8	9	10	11	12
T_x Score	0.0000	1.0000	0.0000	0.0000	0.0000	0.0000	0.0000	0.0000	0.0000	0.0000	0.0000	0.0000
T_y Score	0.0000	0.0000	0.0000	0.0000	1.0000	0.0000	0.0000	0.0000	0.0000	0.0000	0.0000	0.0000
T_z Score	1.0000	0.0000	0.0000	0.0000	0.0000	0.0000	0.0000	0.0000	0.0000	0.0000	0.0000	0.0000

Table A.16: The remaining eigenvalues and corresponding eigenvectors of NO_3^- after removing translation modes

column	1	2	3	4	5	6	7	8	9
eigenvalues	−0.0010	−0.0010	−0.0004	−0.0016	−0.0016	−0.0016	0.0000	0.0000	0.0000
eigenvectors	0.3871	0.0067	0.0000	0.0000	0.0000	0.0000	0.2723	−0.7252	−0.0005
	0.0068	−0.3874	0.0000	0.0001	0.0000	0.0000	−0.7251	−0.2723	−0.0002
	0.0000	0.0000	−0.8660	0.0000	0.0001	0.0000	0.0000	0.0000	0.0000
	−0.2753	0.4931	0.0000	0.4592	0.0000	0.0000	−0.2997	0.0896	−0.3497
	−0.4976	−0.0170	0.0000	0.3498	0.0000	0.0000	0.3936	−0.1177	0.4592
	0.0000	0.0000	0.2887	0.0000	0.5072	−0.6398	0.0000	0.0000	0.0000
	−0.4847	−0.3770	0.0000	−0.5321	0.0000	0.0000	0.1453	0.1369	−0.2231
	0.3724	−0.2264	0.0000	0.2233	0.0000	0.0000	0.3465	0.3265	−0.5320
	0.0000	0.0000	0.2887	0.0000	0.3005	0.7592	0.0000	0.0000	0.0000
	0.3729	−0.1229	0.0000	0.0729	0.0000	0.0000	−0.1180	0.4987	0.5733
	0.1184	0.6308	0.0000	−0.5731	0.0000	0.0000	−0.0150	0.0635	0.0730
	0.0000	0.0000	0.2886	0.0000	−0.8077	−0.1194	0.0000	0.0000	0.0000

Table A.17: The rotation similarity scoring values of NO_3^-

column	1	2	3	4	5	6	7	8	9
R_x Score	0.0000	0.0000	0.0001	0.0000	0.0200	0.9998	0.0000	0.0000	0.0000
R_y Score	0.0000	0.0000	0.0002	0.0000	0.9998	0.0200	0.0000	0.0000	0.0000
R_z Score	0.0002	0.0004	0.0000	1.0000	0.0000	0.0000	0.0000	0.0000	0.0000

Table A.18: The remaining eigenvalues and eigenvectors of NO_3^- that correspond to vibration modes

column	1	2	3	4	5	6
eigenvalues	−0.0010	−0.0010	−0.0004	0.0000	0.0000	0.0000
eigenvectors	0.3871	0.0067	0.0000	0.2723	−0.7252	−0.0005
	0.0068	−0.3874	0.0000	−0.7251	−0.2723	−0.0002
	0.0000	0.0000	−0.8660	0.0000	0.0000	0.0000
	−0.2753	0.4931	0.0000	−0.2997	0.0896	−0.3497
	−0.4976	−0.0170	0.0000	0.3936	−0.1177	0.4592
	0.0000	0.0000	0.2887	0.0000	0.0000	0.0000
	−0.4847	−0.3770	0.0000	0.1453	0.1369	−0.2231
	0.3724	−0.2264	0.0000	0.3465	0.3265	−0.5320
	0.0000	0.0000	0.2887	0.0000	0.0000	0.0000
	0.3729	−0.1229	0.0000	−0.1180	0.4987	0.5733
	0.1184	0.6308	0.0000	−0.0150	0.0635	0.0730
	0.0000	0.0000	0.2886	0.0000	0.0000	0.0000

VITAE

Personal Details

Name   Mr.Chirayut Supunyabut

Place of Birth Udonthani, Thailand

Education

2014-2019   Ph.D. in Chemistry, Chulalongkorn University, Thailand

2011-2013   M.Sc. in Chemistry, Chulalongkorn University, Thailand

2007-2010   B.Sc. in Chemistry, Chulalongkorn University, Thailand

Publication

2020   Supunyabut, C., Paiboonvorachat, N. and Vchirawongkwin, V. Non-Hessian method for normal coordinate calculations: Application to evaluate vibrational spectra. Computational and Theoretical Chemistry 1183 (2020): 112849.